Resources for bosonic metrology: quantum-enhanced precision from a superselection rule perspective

Astghik Saharyan¹, Eloi Descamps¹, Arne Keller^{1,2}, and Pérola Milman^{1*}

¹ Université Paris Cité, CNRS, Laboratoire Matériaux et Phénomènes Quantiques, 75013 Paris, France and

² Départment de Physique, Université Paris-Saclay, 91405 Orsay Cedex, France

Quantum optics and atomic systems are prominent platforms for exploiting quantum-enhanced precision in parameter estimation. However, not only are quantum optical and atomic systems often treated separately, but even within quantum optics, identifying optimal probes (quantum states) and evolutions (parameter-dependent dynamics) typically relies on case-by-case analyses. Mode, and sometimes only particle entanglement, can yield quantum enhancement of precision in continuousand discrete-variable regimes, yet a clear connection between these regimes remains elusive. In this work, we present a unified framework for quantum metrology that encompasses all known precision-enhancing regimes using bosonic resources. We introduce a superselection rule compliant representation of the electromagnetic field that explicitly incorporates the phase reference, enforcing total particle number conservation. This approach provides a description of the electromagnetic field which is formally equivalent to the one employed in atomic systems, and we show how it encompasses both the discrete and the continuous limits of quantum optics. Within this framework, we consistently recover established results while offering a coherent physical interpretation of the quantum resources responsible for precision enhancement. Moreover, we develop general strategies to optimize precision using arbitrary multimode entangled probe states. Finally, our formalism readily accommodates noise, measurement strategies and non-unitary evolutions, extending its applicability to realistic experimental scenarios.

Metrology is one of the few fields where quantum properties can offer advantages over classical protocols [1, 2]. While the precision associated with classical strategies for parameter estimation is fundamentally limited by shot noise - which scales inversely with the square root of resources such as energy and the number of probes - quantum strategies can achieve a quadratic improvement in precision for the same resource budget. Remarkably, unlike many other quantum advantages such as those in quantum computing, quantum metrological protocols are already being implemented across a variety of physical systems, playing key roles in both physics [3–5] and other fields, such as biology [6, 7].

Bosonic systems of diverse types - including single photons [8–11], intense fields [12–19], atomic ensembles [20, 21], and the vibrational modes of trapped ions [22] or of massive oscillators [23] - can be prepared in quantum states that have been theoretically shown, and experimentally demonstrated [24], to enable quantumenhanced precision (QEP), i.e., overcoming the shotnoise. However, depending on the system, the contribution to precision enhancement due to modes, in one hand, and to particle's statistics on the other hand, can differ significantly. For states with well defined particle number where bosons are distributed across orthogonal modes, mode and particle entanglement can be used to achieve QEP [9, 10, 25–27]. In contrast, in the continuousvariable (CV) regime, where states do not necessarily have a definite photon number, strategies based on singlemode states can yield QEP [13–19, 28], though employing ancillary modes can render the implementation of parameter estimation protocols more practical [29]. Finally, a general form of squeezing can also lead to QEP for different physical systems [30].

Despite these numerous successes, a comprehensive framework unifying the diverse regimes of bosonic resources for quantum metrology is still missing. By this we mean a compact, system-independent model from which the metrologically relevant properties of atomic systems and photons - whether in the photon-number-resolved or CV limits, and in both single-mode and multimode regimes [14, 16] - can all be derived and understood as particular instances of a common underlying structure.

In this Letter, we show that explicitly incorporating the phase reference of quantum optical states as a resource - which is often implicit in the CV representation - enables the construction of a general model that unifies the various regimes of bosonic systems used in quantum metrology. Beyond serving as a simple and elegant formal choice, including the phase reference is essential for describing the bosonic field within a framework that respects the photon-number superselection rule (SSR) [31– 41]. We demonstrate how this unified framework naturally recovers known results in both the CV limit and for multimode entangled states with well-defined photon numbers, permitting a clear identification of how different resources contribute to QEP. We show that the general case of noisy, multimode entangled probes can be captured in the provided compact expression. Finally, we use our results to design optimal strategies to maximize the achievable precision and to reach it for arbitrary

We begin by recalling the basic principles of parameter estimation and its associated precision bounds. A metrological protocol starts by preparing a probe - a quantum state $|\psi\rangle$ - whose evolution depends on the parameter

of interest, κ . The estimation precision depends on the choice of probe state, on the parameter-dependent evolution, and on the measurement strategy. It can be quantified using the Fisher information (FI) \mathcal{F}_{κ} , $\delta \kappa \geq 1/\sqrt{\nu \mathcal{F}_{\kappa}}$, with $\mathcal{F}_{\kappa} = \sum_{i} \frac{1}{P_{\kappa}(x_{i})} \left(\frac{\partial P_{\kappa}(x_{i})}{\partial \kappa} \right)^{2}$, where $P_{\kappa}(x_{i})$ is the probability of obtaining an outcome x_{i} that is used to estimate κ for a given measurement strategy and ν the number of measurements. The FI is upper-bounded by the quantum Fisher information (QFI) Q for small parameter variations [42], $\delta \kappa \geq 1/\sqrt{\nu Q}$, that is the optimization of the FI over all possible measurement strategies. For pure-state probes and unitary evolutions $\hat{U} = e^{i\hat{H}\kappa}$, the QFI takes the simple form $Q = 4\Delta^2 \hat{H}$, computed using the probe state $|\psi\rangle$. For non pure states and non-unitary evolutions [43–47], an upper bound for the QFI can be established through purification protocols [48] followed by computing the QFI for such pure states.

The quantum aspects of metrology are particularly appealing when one compares the scaling of precision with some resource, as energy. While in classical protocols this scaling of precision is limited by the shot-noise $(\mathcal{Q} \propto \overline{n})$, where \overline{n} is the intensity of the field or the average number of photons), in quantum metrology precision scaling can display a quadratic enhancement $(\mathcal{Q} \propto \overline{n}^2)$, which is called the Heisenberg scaling.

Numerous strategies have been developed to surpass the shot-noise limit across various types of parameterdependent evolutions. Examples in atomic physics include using spin-squeezed [26, 49, 50], anticoherent [51, 52] and Dicke states [53] as probes in rotation measurements [20, 54, 55]. In quantum optics, entangled photons [5, 25, 56, 57] are often used in phase estimation protocols [58] and applications [59]. Furthermore, single-mode quantum optical states can also achieve QEP in phase estimation and displacement measurements [60– 62. Given this diversity of strategies [63], several questions arise: Are there common underlying principles governing these different approaches? How can one determine whether a given arbitrary state can be an effective probe for a particular type of evolution? And crucially, how can one optimize the precision, given a probe state, when measuring a parameter associated with a specific physical transformation?

Answering these questions requires a deeper analysis of the necessary resources for achieving QEP. It is well established that mode entanglement is not a necessary condition for QEP [64], and that particle entanglement (multimode states) constitutes a key resource for quantum metrological advantage [27, 65], shown to be necessary for QEP for atomic systems [20, 66]. Understanding this requires the introduction of an important formal tool in quantum metrology, which will take on a new significance in the present work: the Schwinger representation [67], which maps two bosonic modes onto angular momentum operators. Creation and anihilation operators in

a mode i are defined as $\hat{a}_i^{\dagger} | n_i \rangle_i = \sqrt{n_i + 1} | n_i + 1 \rangle_i$ and $[\hat{a}_i, \hat{a}_i^{\dagger}] = \delta_{i,j}$. We can then define angular momentum operators $\hat{J}_{x}^{(i,j)} = (\hat{a}_{i}^{\dagger}\hat{a}_{j} + \hat{a}_{i}\hat{a}_{j}^{\dagger})/2, \, \hat{J}_{y}^{(i,j)} = i(\hat{a}_{i}\hat{a}_{j}^{\dagger} - \hat{a}_{i}^{\dagger}\hat{a}_{j})/2$ and $\hat{J}_z^{(i,j)} = (\hat{a}_i^{\dagger} \hat{a}_i - \hat{a}_i^{\dagger} \hat{a}_i)/2$. Angular momentum operators are also used to describe symmetric states of Ntwo-level systems, such as states of Bose-Einstein condensates. In addition, in quantum optics, the Mach-Zehnder interferometer (MZI) - a widely used setup in quantum metrology - can be fully described using such operators: dephasing between modes i and j is represented by an evolution generated by $\hat{J}_z^{(i,j)},$ and beam-splitters correspond to rotations of the form $e^{i\hat{J}_{y}^{(i,j)}\theta}$, where θ is related to the transmissivity of the beam-splitter. Using these tools, a rigorous and detailed comparison between CV path-symmetric states [68] - which admit a particle decomposition, but do not necessarily have a well defined particle number - and states with a fixed number of particles in a first-quantization representation was performed in [27]. The conclusion was that particle entanglement is necessary for surpassing the shot-noise limit in such an interferometric configuration, whereas mode entanglement is not. However, such results are not general as presented, and a clear fundamental connection between the QFI for the considered path-symmetric CV subspaces - or, more generally, for arbitrary CV states - and the QFI for fixed-particle-number states is not established. Consequently, many physically relevant cases are not contemplated, as single-mode squeezed states [12, 19, 69, 70] or Schrödinger cat-like states [60, 62, 71, 72], which can provide precision beyond classical limits for both phase and displacement estimation, even when dynamical evolutions are represented as involving one single mode.

We now provide a general model of resources for bosonic quantum metrology by adopting a SSR compliant (SSRC) representation of the multimode quantum electromagnetic field, that allows the unification and the extension of the previous results within a single, compact formalism.

The usual description of single mode states of electromagnetic field, that we call the CV representation, involves superpositions of Fock states, $|\psi\rangle_1$ $\sum_{n=0}^{\infty} c_n |n\rangle_1$, where subscript 1 denotes an arbitrary mode and $\sum_{n=0}^{\infty} |c_n|^2 = 1$. This representation implicitly supposes a phase reference, otherwise states $|\psi\rangle_1$ should have a well defined total photon number or, instead, be a statistical mixture $\hat{\rho}$ of states with well defined photon number, $[\hat{\rho}, \hat{n}_1] = 0$. In other words, state $|\psi\rangle_1$ does not respect the photon number superselection rule, and it can only correctly represent the field's state when a phase reference is specified or at least implicitly defined. Instead of making such implicit assumptions, one can adopt a SSRC representation of the field, where the phase reference is explicit and treated as a resource. A full discussion on SSR can be found in [39] and its importance for quantum computing and information both in the discrete and continuous limits of quantum optics has been discussed in [40, 41]. Adopting a SSRC representation can also help clarifying the role of modes, states, and resources in general in quantum metrology, as we will now see. As a matter of fact, both the single mode CV and the multimode regimes of bosonic systems are encompassed in the SSRC representation (see also the Supplemental Material for a recap [73]). To show this, we start with the simplest pure state of N photons in the SSRC representation:

$$|\Psi\rangle = \sum_{n=0}^{N} c_n |n\rangle_1 |N - n\rangle_2, \qquad (1)$$

where subscripts 1, 2 denote orthogonal modes that serve as a phase reference to one another. State (1) has a well defined total photon number so coherence is invariant under the free evolution generated by $\hat{H} = \hbar\omega(\hat{n}_1 + \hat{n}_2)$ [74]. The CV limit can be defined using $n_{\text{max}} \leq N/2$ as states for which $\sum_{n=0}^{N} |c_n|^2 n \ll n_{\text{max}}$. Consequently, we mathematically set $n_{\text{max}} \to \infty$ (see [39, 40]), and in this limit, $|\Psi\rangle$ can be expressed as $|\psi\rangle_1$. Such limit is similar to the one discussed in [20, 49, 75], where the Holstein-Primakoff transformation [76] was used. In the present discussion, no approximation is made in (1), N can be arbitrarily large but is finite [77]. It is rather the single mode CV representation that is a sometimes valid representation of bosonic states with a large particle number imbalance between modes. Hence, (1) can be used to represent arbitrary states that become "single mode" ones in the CV limit. The CV limit can also be applied to express multimode states (Eq. (3) in the following) in the CV representation (i.e., two-mode states that do not have a definite number of photons, contrary to (1)), as two-mode squeezed states and the mode-symmetric ones used in [27] (see [73]).

States (1) are formally equivalent to the total angular momentum eigenstates of N 2-level bosonic (symmetric indistinguishable) massive particles, creating a formal equivalence between different physical systems. For all such systems, one can use the results of Ref. [78], that shows that rotations $e^{i\hat{J}_{\vec{n}}^{(1,2)}\xi}$, where $\vec{n}=\cos\beta\vec{z}+$ $\sin \beta \cos \varphi \vec{x} + \sin \beta \sin \varphi \vec{y}$, and the so-called "spin squeezing" operations $e^{i(\hat{J}_{\vec{\pi}}^{(1,2)})^2 \gamma}$, which are often studied in the realm of atomic quantum metrology [79-82], form a universal gate set for symmetric states. Physically, such operators correspond to, respectively, passive Gaussian (rotations) and non-Gaussian (spin squeezing) [83, 84] operations in the quadrature space [85] in the CV limit. Rotations generated by $\hat{J}_z^{(1,2)}$ can be used to describe the dephasing between two modes due to the free evolution (as for instance in a MZI), and $\hat{J}_x^{(1,2)}$ and $\hat{J}_y^{(1,2)}$ represent the action of a beam-splitter. Finally, the spin squeezing operation is a non-linear Kerr-like effect, and this type of non-linear evolution can be essential for parameter estimation in some relevant interacting bosonic systems [86].

In the SSRC representation, these operators gain a different status for forming a universal gate set, replacing [87] which is restricted to the CV limit. In addition, the applicability of the SSRC universal gate set is not anymore restricted to the description of specific physical set-ups - as the MZI -, since gates from the universal set can be combined to express, with arbitrary precision, any unitary transformation applied to a field's state.

Using these results, we now discuss the different limits of quantum metrology starting from (1) and its multimode versions. For this, we consider a general rotation, $e^{i\hat{J}_{\vec{n}}^{(1,2)}\xi} = e^{i\hat{J}_{z}^{(1,2)}\phi}e^{i\hat{J}_{y}^{(1,2)}\theta}$, i.e., a combination of a beam-splitter and a dephasing. This operation is a mode basis transformation that does not create particle entanglement [41, 66, 88] and can, in particular, be used to describe the equivalence between Fock states and coherent states that will be useful here: $\lim_{N\to\infty}(\cos\left(\frac{\theta}{2}\right)\hat{a}_2^{\dagger}+$ $e^{i\phi}\sin\left(\frac{\theta}{2}\right)\hat{a}_{1}^{\dagger})^{N}/\sqrt{N!}\left|\emptyset\right\rangle = (\hat{a}_{\theta,\phi}^{\dagger})^{N}/\sqrt{N!}\left|\emptyset\right\rangle = |N\rangle_{\theta,\phi} \rightarrow$ $|\alpha\rangle_1$ with $\alpha = e^{i\phi}\sin\left(\frac{\theta}{2}\right)\sqrt{N}$, as shown in [40, 41] and [73]. In the metrology scenario, one might be interested in estimating the parameters ϕ , θ or ξ above. In (4) of the End Matter we show the QFI when estimating ξ using a general probe state as (1), from which the estimation of θ and ϕ can be derived with a proper choice of \vec{n} . We now focus on estimating θ (rotations around y, $\beta = \pi/2$, $\varphi = \pi/2$). The CV limit (large N) corresponds to restricting states and evolutions to the tangent plane to the Bloch sphere [20] (see [73]). By setting $\theta/2 = |\alpha|/\sqrt{N}$, $\theta \ll 1$ in the CV limit (large N), rotations around directions in the x,y plane correspond to a finite displacement $|\alpha|$. Consequently, the precision in estimating $|\alpha|$ is:

$$\delta\left(\frac{\theta}{2}\right) = \frac{\delta|\alpha|}{\sqrt{N}} \ge \frac{1}{\sqrt{4\nu\Delta^2\hat{J}_y}}.$$
 (2)

Inspecting Eq. (6) of the End Matter, we see that, interestingly, in the CV limit, the scaling of precision depends only on the population of mode 1, even though the evolution operator $\hat{J}_y^{(1,2)}$ explicitly includes both modes. These results, which are valid for arbitrary states in the CV limit, are compatible with the ones obtained using the Holstein-Primakoff approximation [89] and with the fact that rotations around directions x, y become translations in the quadrature space [40]. Nevertheless, in the present picture, we applied constraints to the states and parameters of evolutions rather than to the operators, so as to keep the framework as general as possible. Notice that the scaling of precision on measuring θ can reach the Heisenberg limit $\propto 1/N$. However, the constraints to small angles in the CV representation modifies the scaling of the QFI from $\propto N^2$ to linear in the average photon number in mode 1, \overline{n} (see End Matter).

We can also analyze rotations around the z axis, which correspond to rotations in phase space in the CV limit. Now, the rotation angle can be arbitrary and irrespectively of the considered limit, precision depends only on the number of photons in mode 1. However, in the CV limit, this corresponds to, at most, a quadratic scaling of the QFI with \overline{n} (as compared to a quadratic scaling in N that is in principle possible for states in the form (1)). As a conclusion, the SSRC representation permits a unified picture of the QFI for atoms and photons in any photon number regime, explicitly using two modes that serve as a phase reference to one another. While in the cases where there is a photon number balance between the two modes the total photon number N can be treated as a resource, in the CV limit, when there is an imbalance between the modes, one can consider a single mode evolution even though both modes are being manipulated, and the considered resource is \overline{n} .

This "replacement" of N by \overline{n} in the CV limit has in fact important physical implications on how modes and states function as resources in metrology, that are revealed by the presented formalism. In order to illustrate this, we will focus on two paradigmatic examples for quantum metrology, the NOON state and the Schrödinger cat state. These states are often compared in the literature [90-94] and lead to a quadratic enhancement in precision with respect to the shot noise. While NOON states are two mode states of the type $|\mathcal{N}\rangle = \frac{1}{\sqrt{2}}(|N\rangle_1|0\rangle_2 + |0\rangle_1|N\rangle_2$, where $|N\rangle_i$ is a Fock state with N photons in mode i, Schrödinger cat-like states in the CV representation are superpositions of single mode coherent states, $|\mathcal{C}\rangle = \frac{1}{\mathcal{K}}(|0\rangle_1 + |\alpha\rangle_1)$, where $|\alpha\rangle_1$ is a coherent state, for which $\overline{n} = |\alpha|^2$, and \mathcal{K} the normalization. Usually, the QFI is computed for these states using an evolution generated by $\hat{H} \propto \hat{n}_1$, and it leads, respectively to $Q_N \propto N^2$ for $|N\rangle$ and $Q_{\mathcal{C}} \propto |\alpha|^4 (1 - e^{-2|\alpha|^2})$ for $|\mathcal{C}\rangle$, i.e., both states permit reaching the Heisenberg scaling for $|\alpha|^2 = \overline{n} \gg 1$. However, in the SSRC formalism, states $|\mathcal{C}\rangle$ are the large N limit of the states studied in [95]: up to a normalization factor, $|N\rangle_2 + |N\rangle_{\theta,\phi} \rightarrow |0\rangle_1 + |\alpha\rangle_1$ in the CV limit (see [73]). Moreover, the generator of the evolution for both states is actually a two-mode operator $\hat{J}_z^{(1,2)}$ acting on the CV "single-mode" state (mode 1) and the phase reference (mode 2). Finally, the resources used in both states are entirely different. While the scaling of the NOON state depends on the total number of photons in the two modes, N, the one of $|\mathcal{C}\rangle$ depends on the number of photons in mode 1, which is actually related, for fixed N, to the mode overlap [84]: $[\hat{a}_2, \hat{a}_{\theta,\phi}^{\dagger}] = \cos \frac{\theta}{2} = \sqrt{1 - |\alpha|^2/N}$.

We conclude by showing that the SSRC representation enables a compact description of parameter estimation using general multimode states as probes, possibly nonpure. For this, we will study a state that can correspond to two-mode state in the CV limit:

$$\prod_{\substack{i,j=1\\i< j}}^{4} \hat{U}_{i,j} \sum_{\substack{n_1,n_2=0\\n_1+n_2 \le N}} c_{n_1,n_2} |n_1\rangle_1 |n_2\rangle_2 |N-n_1-n_2\rangle_3 |0\rangle_4.$$

In (3), modes 1, 2 and 3 are the probes (that reduce to modes 1 and 2 with 3 serving as a phase reference in the CV limit), and mode 4 can play the role of the environment. It is common to model the interaction between the probe and the environment as a beam-splitter [48] and trace out mode 4 so as to obtain a non-pure probe or a non-unitary evolution of the probe. This procedure is of course possible in the present description, where we can also consider the environment initial state different from the vacuum, which would complicate the description without any significant qualitative change. Hence, the coupling to the environment can be modeled by the unitary operation $\hat{U}_{i,4} = e^{i\hat{J}_x^{(i,4)}\kappa_i}$, where $i \in \{1,2,3\}$ and κ_i is a parameter related to the coupling strength between system and environment (as the photon absorption rate of a material [48, 96]) and we considered a specific coupling to the environment associated with the evolution \hat{J}_x without loss of generality. Alternatively, mode 4 can represent an ancillary mode that enables the implementation of generalized measurements, and we establish conditions for which $\mathcal{F}_{\kappa} = \mathcal{Q}$ for pure or mixed states that include those discussed in [97, 98]. We show in [73] the working principles of such a generalized interferometer.

We now show how our framework enables a systematic optimization of the state and mode resources for parameter estimation, given an arbitrary initial probe state. The dependence of the QFI on modal structure for general states in the CV limit has been analyzed in [99], where mode optimization strategies were developed without affecting the scaling of the achievable precision. In addition, optimal rotation directions for symmetric states were identified in [100]. Here, we address a different problem: starting from a general probe state as Eq. (3), where the unitary operator $\prod_{1 < i < j < 3} \hat{U}_{i,j}$ encodes a physical transformation - such as a rotation around a known axis \vec{n} - we aim to determine how the generator of the evolution should act on the different modes so as to maximize the QFI. For instance, in the absence of noise and losses, $\hat{U}_{i,j} = e^{i\hat{J}_{\vec{n}}^{(i,j)}\theta_{i,j}}$. This evolution represents a dephasing or a translation (in the CV limit), and may involve various combinations of probe modes (i, j = 1, 2, 3) depending on the relative weights of $\theta_{i,j}$. Different relative weights define different modes, as we will see in the following. The central question is: given an arbitrary initial probe state in the SSRC representation - whether corresponding to single- or multimode, entangled or separable, CV or with fixed particle number - how should the evolution generator exploit the probe's modal structure to maximize the QFI? In practical terms: what is the optimal choice of the relative weights of $\theta_{i,j}$, given the probe state and the generator direction \vec{n} ?

To illustrate our method (see Supplementary Material [73] for the general treatment), we focus on the case of phase estimation $(\vec{n} = \vec{z})$. We set $\theta_{1,2} = 0$ for simplicity, so $\prod_{i,j=1}^{3} \hat{U}_{i,j} = e^{i\frac{1}{2}(\theta_{1,3}\hat{n}_1 + \theta_{2,3}\hat{n}_2 - (\theta_{1,3} + \theta_{2,3})\hat{n}_3)}$. Defining

ing $\hat{n}_{\zeta} = \cos\zeta\,\hat{n}_1 + \sin\zeta\,\hat{n}_2$ and its orthogonal counterpart $\hat{n}_{\zeta_{\perp}} = \sin\zeta\,\hat{n}_1 - \cos\zeta\,\hat{n}_2$, so $\theta\hat{n}_{\zeta} = \theta_{1,3}\hat{n}_1 + \theta_{2,3}\hat{n}_2$. Typically, only modes 1 and 2 are directly measured in the CV limit, and the QFI associated with estimating θ is $4\Delta^2\hat{n}_{\zeta}$. Because the total variance satisfies $\Delta^2\hat{n}_1 + \Delta^2\hat{n}_2 = \Delta^2\hat{n}_{\zeta} + \Delta^2\hat{n}_{\zeta_{\perp}}$, it follows that the optimal strategy is to choose ζ - i.e., the relative weights of $\theta_{1,3}$ and $\theta_{2,3}$ - so as to maximize $\Delta^2\hat{n}_{\zeta}$, or equivalently minimize $\Delta^2\hat{n}_{\zeta_{\perp}}$.

For instance, consider two-mode maximally correlated states of the form $\sum_{\substack{n=0\\2n\leq N}}^{N}c_n\left|n\right\rangle_1\left|n\right\rangle_2\left|N-2n\right\rangle_3$, as in the case of two-mode squeezed states in the CV limit. The optimal strategy is to choose $\zeta=\pi/4$, for which $\Delta^2\hat{n}_{\zeta_\perp}=0$. The (mode-dependent) estimated parameter is then $\theta_+/2=(\theta_{1,3}+\theta_{2,3})/\sqrt{2}$. Notably, although the phase reference mode (mode 3) is not directly measured - and the QFI does not explicitly depend on its properties in the CV limit as previously discussed - its presence is essential, since phases are defined relative to this mode.

The optimization of the QFI for a k-mode maximally correlated state $\sum_{\substack{n=0\\2n\leq N}}^{N} c_n |n\rangle_1 |n\rangle_2 \dots |N-kn\rangle_{k+1}$ leads to $\mathcal{Q}=4(k+1)^2\Delta^2\hat{n}$, where $\Delta^2\hat{n}$ is the single mode variance [73]. The quadratic mode scaling, irrespectively of the photon-number variance, illustrates the intricate interplay between entanglement and coherence in QEP. A notable example are multimode-entangled single-photon states discussed in [9, 10, 46, 101–104]. Finally, the optimization procedure applies to different rotation axis, which lead, in particular, to the optimization of mode displacement in the CV limit. These examples are developed in [73].

As a conclusion, we have presented a unified and general model that encompasses all known regimes of bosonic quantum metrology, covering symmetric atomic systems and photonic systems alike, in both single and multimode configurations, and in both fixed-photon-number and CV limits. Our framework incorporates noisy dynamics, general non-unitary evolutions, and the formal description of optimal measurement strategies, while also generalizing previous results that identify particle entanglement as a key resource for QEP. A central element enabling this unification is the SSRC description of the field, which enforces total particle number conservation and reveals the conditions for coherence between different symmetric states. Beyond its compactness and generality, we showed that our formalism can be used to optimize the QEP for arbitrary probes, including multimode ones with an arbitrary number of photons in each mode in the CV limit. Specifically, it shows that sometimes measuring observables associated with collective operators enables optimal precision - a strategy directly analogous to those employed to detect entanglement in multimode probes involving atomic and photonic systems [10, 81, 82, 101, 105–107].

ACKNOWLEDGEMENTS

We acknowledge funding from the Plan France 2030 through the project ANR-22-PETQ-0006. We are also indebted to N. Fabre, N. Moulonguet and J. D. Diaz Martinez for inspiring discussions.

END MATTER

General expression for the variance

The general expression of the variance $\Delta^2 \hat{J}_{\vec{n}}$, $\vec{n} = \cos \beta \vec{z} + \sin \beta \cos \varphi \vec{x} + \sin \beta \sin \varphi \vec{y}$ for an arbitrary pure SSRC state (as (1)) is given by

$$\Delta^{2} \hat{J}_{\vec{n}} = \frac{N}{4} \sin^{2} \beta + \frac{1}{2} \left(N \overline{n} - \overline{n^{2}} \right) \sin^{2} \beta + \Delta^{2} n \cos^{2} \beta - \left(\sum_{n=0}^{N-1} \operatorname{Re} \{ c_{n} c_{n+1}^{*} e^{-i\varphi} \} \sqrt{(n+1)(N-n)} \right)^{2} \sin^{2} \beta + \frac{1}{2} \sum_{n=0}^{N-2} \operatorname{Re} \{ c_{n} c_{n+2}^{*} e^{-2i\varphi} \} \times \sqrt{(N-n)(N-n-1)(n+1)(n+2)} \sin^{2} \beta + \frac{1}{2} \sum_{n=0}^{N-1} \operatorname{Re} \{ c_{n} c_{n+1}^{*} e^{-i\varphi} \} (2n-2\overline{n}+1) \times \sqrt{(N-n)(n+1)} \cos \beta \sin \beta,$$
(4)

where $\Delta^2 n = \overline{n^2} - \overline{n}^2$, with $\overline{n^2} = \sum_{n=0}^N |c_n|^2 n^2$ and $\overline{n} = \sum_{n=0}^N |c_n|^2 n$.

The CV limit of rotations around the x axis (phase-space translations)

Rotations around the axis \vec{y} correspond to setting $\beta = \pi/2$ and $\varphi = \pi/2$, so defining $\theta/2 = |\alpha|/\sqrt{N}$ as in the main text, we have that

$$\delta\left(\frac{\theta}{2}\right) = \frac{\delta|\alpha|}{\sqrt{N}} \ge \frac{1}{\sqrt{4\nu\Delta^2 \hat{J}_y}},\tag{5}$$

where, using (4)

$$\Delta^{2} \hat{J}_{y} = \frac{N}{4} + \frac{1}{2} \left(N \overline{n} - \overline{n^{2}} \right) - \left(\sum_{n=0}^{N-1} \operatorname{Re} \{ -i c_{n} c_{n+1}^{*} \} \sqrt{(n+1)(N-n)} \right)^{2} + \frac{-1}{2} \sum_{n=0}^{N-2} \operatorname{Re} \{ c_{n} c_{n+2}^{*} \} \times \sqrt{(N-n)(N-n-1)(n+1)(n+2)}.$$
 (6)

When considering $\delta |\alpha|$ and $\overline{n}/N \to 0$ (which is the relevant precision in the CV limit), we have that $\overline{n}/N \to 0$, $\overline{n^2}/N \to 0$ and

$$\delta|\alpha| \ge \frac{1}{\sqrt{4\nu\Delta^2\hat{p}}},\tag{7}$$

with $\hat{p} = \frac{i}{2}(\hat{a}_1 - \hat{a}_1^{\dagger})$. We see that the dependency on N of $\Delta^2 \hat{J}_y$ disappears. At most, one can expect a linear scaling of precision with \overline{n} .

The CV limit of rotations around the z axis (phase-space rotations)

In the CV limit, states are restricted to a tangent, but rotations around the z axis ($\sin \beta = 0$ and $\cos \beta = 1$) can be of any angle. Eq. (4) then becomes:

$$\Delta^2 \hat{J}_z = \Delta^2 \hat{n}. \tag{8}$$

The interest of this results is that it does not depend on the rotation direction or on the CV limit (value of N).

From the SSRC representation to coherent states

In this section we show how to extract a CV coherent state (Glauber coherent state) $|\alpha\rangle_a$ ($\alpha\in\mathbb{C}$) in a mode a from a Fock state $|N\rangle_b$ in an orthogonal mode b. We will see that it requires to consider the $N\to\infty$. The two modes beeing orthogonal their respective anhibitation and creation operator fulfill $[\hat{a}, \hat{b}^{\dagger}] = 0$. We fix $\alpha\in\mathbb{C}$. We consider an N-and- α -dependent linear transformation \hat{U} of the mode given by

$$\hat{U}\hat{a}^{\dagger}\hat{U}^{\dagger} = \sqrt{1 - \frac{\left|\alpha\right|^2}{N}}\hat{a}^{\dagger} - \frac{\alpha^*}{\sqrt{N}}\hat{b}^{\dagger} \qquad \qquad \hat{U}\hat{b}^{\dagger}\hat{U}^{\dagger} = \frac{\alpha}{\sqrt{N}}\hat{a}^{\dagger} + \sqrt{1 - \frac{\left|\alpha\right|^2}{N}}\hat{b}^{\dagger}.$$

The transformation \hat{U} is a rotation $\hat{R}(\theta,\phi)(\alpha,N) = e^{i\phi\hat{J}_z}e^{i\theta\hat{J}_y}$ with parameters $\theta(\alpha,N) = 2\arccos\left(\sqrt{1-\frac{|\alpha|^2}{N}}\right)$ and $\phi(\alpha,N) = \arg(\alpha)$. A quick computation allows us to verify that $[\hat{U}\hat{a}^\dagger\hat{U}^\dagger,\hat{U}\hat{b}^\dagger\hat{U}^\dagger] = 0$, such that it indeed corresponds to a unitary transformation. We can now consider in the limit of $N \to \infty$ the state $\hat{U}|N\rangle_b$

$$\hat{U}|N\rangle_b = \frac{(\hat{U}\hat{b}^{\dagger}\hat{U}^{\dagger})^N}{\sqrt{N!}}|\emptyset\rangle \tag{9a}$$

$$= \frac{1}{\sqrt{N!}} \left(\frac{\alpha}{\sqrt{N}} \hat{a}^{\dagger} + \sqrt{1 - \frac{|\alpha|^2}{N}} \hat{b}^{\dagger} \right)^N |\emptyset\rangle \tag{9b}$$

$$= \frac{1}{\sqrt{N!}} \sum_{k=0}^{N} {N \choose k} \frac{\alpha^k}{\sqrt{N}^k} \sqrt{1 - \frac{|\alpha|^2}{N}}^{N-k} (a^{\dagger})^k (\hat{b}^{\dagger})^{N-k} |\emptyset\rangle$$
(9c)

$$=\sum_{k=0}^{N} {N \choose k} \frac{\sqrt{k!}\sqrt{(N-k)!}}{\sqrt{N!}} \frac{\alpha^k}{\sqrt{N^k}} \sqrt{1 - \frac{|\alpha|^2}{N}}^{N-k} |k\rangle_a |N-k\rangle_b$$
(9d)

$$=\sum_{k=0}^{N}\sqrt{\frac{N(N-1)\cdots(N-k+1)}{k!}}\frac{\alpha^{k}}{\sqrt{N^{k}}}\sqrt{1-\frac{|\alpha|^{2}}{N}}^{N}\sqrt{1-\frac{|\alpha|^{2}}{N}}^{-k}|k\rangle_{a}|N-k\rangle_{b}$$
(9e)

$$\simeq \sum_{k=0}^{N} \frac{\sqrt{N}^k}{\sqrt{k!}} \frac{\alpha^k}{\sqrt{N}^k} e^{-|\alpha|^2/2} |k\rangle_a |N - k\rangle_b \tag{9f}$$

$$=e^{-|\alpha|^2/2}\sum_{k=0}^{N}\frac{\alpha^k}{\sqrt{k!}}|k\rangle_a|N-k\rangle_b.$$
(9g)

Where the approximation is considered term by term: k is fixed while $N \to \infty$.

$$N(N-1)\cdots(N-k+1) \simeq N^k$$
 $\sqrt{1-\frac{|\alpha|^2}{N}}^N \simeq e^{-|\alpha|^2/2}$ $\sqrt{1-\frac{|\alpha|^2}{N}}^k \simeq 1.$ (10)

Parameter estimation for multimode SSRC state

In the following, we demonstrate how, starting from a multimode SSRC state one can optimize the quantum Fisher information (QFI) associated with generators acting on different modes, but all associated with a same given rotation axis \vec{n} . For instance, when $\vec{n} = \vec{z}$ we are analyzing phase estimation using multimode rotations, and this can be done in different ways given a general multimode bosonic state, *i.e.*, by differently manipulating each mode so as to optimize precision when measuring a parameter that controls the collective evolution, as will be seen later in this section. This analysis highlights the role of mode structure and correlations between them in enhancing precision, a procedure directly related to entanglement detection using collective variables studied in [101].

We start by considering a general three-mode state conserving the total number of particles N, of the form:

$$|\psi\rangle = \sum_{\substack{n_1, n_2 = 0\\n_1 + n_2 \le N}}^{N} c_{n_1, n_2} |n_1\rangle_1 |n_2\rangle_2 |N - (n_1 + n_2)\rangle_3.$$
(11)

This state undergoes pairwise rotations generated by $\hat{J}_z^{(i,j)}$, that encode parameters $\theta_{i,j}$:

$$\hat{U} = \prod_{\substack{i,j=1\\i < j}}^{3} \hat{U}_{i,j} = \prod_{\substack{i,j=1\\i < j}}^{3} e^{i\hat{J}_{z}^{(i,j)}\theta_{i,j}},$$

and the transformed state becomes

$$|\tilde{\psi}\rangle = \hat{U}|\psi\rangle = \prod_{\substack{i,j=1\\i < j}}^{3} e^{i\hat{J}_{z}^{(i,j)}\theta_{i,j}}|\psi\rangle = e^{\frac{i}{2}(\hat{n}_{1}(\theta_{1,3}+\theta_{1,2})+\hat{n}_{2}(\theta_{2,3}-\theta_{1,2})-\hat{n}_{3}(\theta_{2,3}+\theta_{1,3}))}|\psi\rangle. \tag{12}$$

To find each bimodal generator that can be combined to optimize the QFI associated with the estimation of a parameter governing a collective evolution, we start by computing the QFI associated with the general evolution (12). This can be done by parametrizing the rotation angles $\theta_{i,j}$ such that the transformation \hat{U} of eq. (12) becomes equivalent to a global phase evolution under an effective generator $\hat{\kappa}_3$. To do so we define the following operators:

$$\hat{\kappa}_3 = \cos \phi_2 \hat{n}_3 + \sin \phi_2 \left(\cos \phi_1 \hat{n}_2 + \sin \phi_1 \hat{n}_1 \right), \tag{13a}$$

$$\hat{\kappa}_2 = \sin \phi_2 \hat{n}_3 - \cos \phi_2 \left(\cos \phi_1 \hat{n}_2 + \sin \phi_1 \hat{n}_1 \right), \tag{13b}$$

$$\hat{\kappa}_1 = \sin \phi_1 \hat{n}_2 - \cos \phi_1 \hat{n}_1,\tag{13c}$$

where the parameters ϕ_i and ζ can be defined as

$$(\theta_{1,3} + \theta_{1,2}) = \zeta \sin \phi_1 \sin \phi_2, \tag{14a}$$

$$(\theta_{2,3} - \theta_{1,2}) = \zeta \sin \phi_2 \cos \phi_1, \tag{14b}$$

$$(\theta_{2,3} + \theta_{1,3}) = -\zeta \cos \phi_2. \tag{14c}$$

With these definitions the expression in Eq. (12) becomes

$$\hat{U}|\psi\rangle = \prod_{\substack{i,j=1\\i < j}}^{3} e^{i\hat{J}_{z}^{(i,j)}\theta_{i,j}}|\psi\rangle = e^{i\frac{\zeta}{2}\hat{\kappa}_{3}}|\psi\rangle. \tag{15}$$

Thus, the effective generator for the collective transformation involving different mode rotations around the same axis is given by $\hat{\kappa}_3$. To maximize the precision for estimating $\zeta/2$, we therefore want to maximize the variance $\Delta^2\hat{\kappa}_3$ of this generator, leading to the quantum Cramér-Rao bound:

$$\delta\left(\frac{\zeta}{2}\right) \geq \frac{1}{\sqrt{\nu\mathcal{Q}}} = \frac{1}{\sqrt{4\nu\Delta^2\hat{\kappa}_3}},$$

where $Q = 4\Delta^2 \hat{\kappa}_3$ is the quantum Fisher information (QFI), and ν denotes the number of independent measurements. For readability, we will omit ν in what follows.

With the definitions in eq. (13), we have the following constraint on the total variance

$$\Delta^2 \hat{\kappa}_3 + \Delta^2 \hat{\kappa}_2 + \Delta^2 \hat{\kappa}_1 = \Delta^2 \hat{n}_1 + \Delta^2 \hat{n}_2 + \Delta^2 \hat{n}_3. \tag{16}$$

This implies that the total variance $\Delta^2 \hat{\kappa}_3 + \Delta^2 \hat{\kappa}_2 + \Delta^2 \hat{\kappa}_1$ is fixed. This sets an upper bound on the achievable QFI, and shows that the maximum precision attainable for estimating ζ – which corresponds to maximizing $\Delta^2 \hat{\kappa}_3$ – is achieved when $\Delta^2 \hat{\kappa}_2 + \Delta^2 \hat{\kappa}_1 = 0$, and is determined by $\Delta^2 \hat{\kappa}_3 = \Delta^2 \hat{n}_1 + \Delta^2 \hat{n}_2 + \Delta^2 \hat{n}_3$. Notice that satisfying these conditions is not always possible, and in this case, one can always minimize the sums of variances. In practice, this means choosing the collective transformation $\hat{\kappa}_3$ such that the combined three-mode state has largest collective variance fixed by $\Delta^2 \hat{n}_1 + \Delta^2 \hat{n}_2 + \Delta^2 \hat{n}_3$. We can explicit the variances as follows:

$$\Delta^{2}\hat{\kappa}_{3} = \cos^{2}\phi_{2}\Delta^{2}\hat{n}_{3} + \sin^{2}\phi_{2}\cos^{2}\phi_{1}\Delta^{2}\hat{n}_{2} + \sin^{2}\phi_{2}\sin^{2}\phi_{1}\Delta^{2}\hat{n}_{1} + 2\sin^{2}\phi_{2}\sin\phi_{1}\cos\phi_{1}\operatorname{Cov}\{\hat{n}_{1}\hat{n}_{2}\}$$

$$+ 2\sin\phi_{2}\cos\phi_{2}\cos\phi_{1}\operatorname{Cov}\{\hat{n}_{3}\hat{n}_{2}\} + 2\sin\phi_{2}\cos\phi_{2}\sin\phi_{1}\operatorname{Cov}\{\hat{n}_{3}\hat{n}_{1}\},$$

$$(17a)$$

$$\Delta^{2}\hat{\kappa}_{2} = \sin^{2}\phi_{2}\Delta^{2}\hat{n}_{3} + \cos^{2}\phi_{2}\cos^{2}\phi_{1}\Delta^{2}\hat{n}_{2} + \cos^{2}\phi_{2}\sin^{2}\phi_{1}\Delta^{2}\hat{n}_{1} + 2\cos^{2}\phi_{2}\sin\phi_{1}\cos\phi_{1$$

$$\Delta^{2}\hat{\kappa}_{1} = \sin^{2}\phi_{1}\Delta^{2}\hat{n}_{2} + \cos^{2}\phi_{1}\Delta^{2}\hat{n}_{1} - 2\sin\phi_{1}\cos\phi_{1}\text{Cov}\{\hat{n}_{1}\hat{n}_{2}\},\tag{17c}$$

with

$$\Delta^{2}\hat{n}_{i} = \overline{n_{i}^{2}} - \overline{n}_{i}^{2}; \quad \overline{n_{i}^{2}} = \sum_{\substack{n_{1}, n_{2} = 0 \\ n_{1} + n_{2} \leq N}}^{N} |c_{n_{1}, n_{2}}|^{2} n_{i}^{2}; \quad \overline{n}_{i} = \sum_{\substack{n_{1}, n_{2} = 0 \\ n_{1} + n_{2} \leq N}}^{N} |c_{n_{1}, n_{2}}|^{2} n_{i};$$

$$\operatorname{Cov}\{\hat{n}_{i}, \hat{n}_{j}\} = \sum_{\substack{n_{1}, n_{2} = 0 \\ n_{1} + n_{2} \leq N}}^{N} |c_{n_{1}, n_{2}}|^{2} n_{i} n_{j} - \overline{n}_{i} \overline{n}_{j}.$$

Additionally, using the fact that the total photon number is conserved, i.e., $n_3 = N - (n_1 + n_2)$, we obtain the following relations:

$$\begin{split} \Delta^2 \hat{n}_3 &= \Delta^2 \hat{n}_1 + \Delta^2 \hat{n}_2 + 2 \mathrm{Cov} \{ \hat{n}_1 \hat{n}_2 \}, \\ \mathrm{Cov} \{ \hat{n}_3 \hat{n}_2 \} &= -\Delta^2 \hat{n}_2 - \mathrm{Cov} \{ \hat{n}_1 \hat{n}_2 \}, \\ \mathrm{Cov} \{ \hat{n}_3 \hat{n}_1 \} &= -\Delta^2 \hat{n}_1 - \mathrm{Cov} \{ \hat{n}_1 \hat{n}_2 \}. \end{split}$$

With these, the expressions in eq. (17) become:

$$\Delta^{2} \hat{\kappa}_{3} = (\cos \phi_{2} - \sin \phi_{2} \sin \phi_{1})^{2} \Delta^{2} \hat{n}_{1} + (\cos \phi_{2} - \sin \phi_{2} \cos \phi_{1})^{2} \Delta^{2} \hat{n}_{2}$$

$$+ 2 \operatorname{Cov} \{ \hat{n}_{1} \hat{n}_{2} \} \left(\cos^{2} \phi_{2} + \sin^{2} \phi_{2} \sin \phi_{1} \cos \phi_{1} - \sin \phi_{2} \cos \phi_{2} \left(\cos \phi_{1} + \sin \phi_{1} \right) \right)$$
(18a)

$$\Delta^{2} \hat{\kappa}_{2} = (\cos \phi_{2} \cos \phi_{1} + \sin \phi_{2})^{2} \Delta^{2} \hat{n}_{2} + (\sin \phi_{2} + \cos \phi_{2} \sin \phi_{1})^{2} \Delta^{2} \hat{n}_{1} + 2 \text{Cov} \{\hat{n}_{1} \hat{n}_{2}\} (\sin^{2} \phi_{2} + \cos^{2} \phi_{2} \sin \phi_{1} \cos \phi_{1} + \sin \phi_{2} \cos \phi_{2} (\sin \phi_{1} + \cos \phi_{1}))$$
(18b)

$$\Delta^{2}\hat{\kappa}_{1} = \sin^{2}\phi_{1}\Delta^{2}\hat{n}_{2} + \cos^{2}\phi_{1}\Delta^{2}\hat{n}_{1} - 2\sin\phi_{1}\cos\phi_{1}\operatorname{Cov}\{\hat{n}_{1}\hat{n}_{2}\}.$$
(18c)

Using Eq. (16), we can compute the total variance:

$$\Delta^2 \hat{\kappa}_3 + \Delta^2 \hat{\kappa}_2 + \Delta^2 \hat{\kappa}_1 = 2\Delta^2 \hat{n}_1 + 2\Delta^2 \hat{n}_2 + 2\text{Cov}\{\hat{n}_1 \hat{n}_2\}.$$
 (19)

The precision bound for estimating ζ becomes

$$\delta\left(\frac{\zeta}{2}\right) \ge \frac{1}{\sqrt{4\Delta^2 \hat{\kappa}_3}} = \frac{1}{\sqrt{4\left(2\Delta^2 \hat{n}_1 + 2\Delta^2 \hat{n}_2 + 2\text{Cov}\{\hat{n}_1 \hat{n}_2\}\right)}}.$$
 (20)

This expression shows that the precision depends not only on the photon number variance in each mode but also on their mutual correlations, as expected in the multimode configuration. Nevertheless, such correlations can be casted as the measurement of a single collective mode defined in terms of modes 1, 2 and 3 (Eq. (13a)).

We now study as an illustrative example the particular state in which $n_1 = n_2 = n$, *i.e.*, the first two modes are maximally correlated, containing the same number of photons, while the reference mode is occupied by N-2n photons, *i.e.*, a state in the general form $|\psi\rangle = \sum_{n=0}^{N/2} c_n |n\rangle_1 |n\rangle_2 |N-2n\rangle_3$. In this case, expression (19) simplifies to

$$\Delta^2 \hat{\kappa}_3 + \Delta^2 \hat{\kappa}_2 + \Delta^2 \hat{\kappa}_1 = 6\Delta^2 \hat{n},\tag{21}$$

where $\hat{n} = \frac{1}{2}(\hat{n}_1 + \hat{n}_2)$. Thus, we can maximize $\Delta^2 \hat{\kappa}_3$ by minimizing $\Delta^2 \hat{\kappa}_2 + \Delta^2 \hat{\kappa}_1$, with the maximum value being fixed by $6\Delta^2 \hat{n}$. For such a state, the variances defined in eq. (18) read as follows:

$$\Delta^2 \hat{\kappa}_3 = (2\cos\phi_2 - \sin\phi_2(\sin\phi_1 + \cos\phi_2))^2 \Delta^2 \hat{n}$$
(22a)

$$\Delta^2 \hat{\kappa}_2 = (2\sin\phi_2 + \cos\phi_2 (\sin\phi_1 + \cos\phi_1))^2 \Delta^2 \hat{n}$$
(22b)

$$\Delta^2 \hat{\kappa}_1 = \left(\sin \phi_1 - \cos \phi_1\right)^2 \Delta^2 \hat{n}. \tag{22c}$$

In order to minimize $\Delta^2 \hat{\kappa}_2 + \Delta^2 \hat{\kappa}_1$, we first choose $\sin \phi_1 = \cos \phi_1 = 1/\sqrt{2}$, which gives:

$$\Delta^2 \hat{\kappa}_3 = \left(\sqrt{2}\cos\phi_2 - \sin\phi_2\right)^2 2\Delta^2 \hat{n}$$
$$\Delta^2 \hat{\kappa}_2 = \left(\sqrt{2}\sin\phi_2 + \cos\phi_2\right)^2 2\Delta^2 \hat{n}$$
$$\Delta^2 \hat{\kappa}_1 = 0.$$

Next, by choosing the parameters such that

$$\sqrt{2}\sin\phi_2 = -\cos\phi_2,$$
$$\sin\phi_2 = \frac{1}{\sqrt{3}}$$

we finally obtain:

$$\Delta^{2}\hat{\kappa}_{3} = \left(\sqrt{2} + \frac{1}{\sqrt{2}}\right)^{2}\cos^{2}\phi_{2}2\Delta^{2}\hat{n} = 9\cos^{2}\phi_{2}\Delta^{2}\hat{n} = 6\Delta^{2}\hat{n}$$

$$\Delta^{2}\hat{\kappa}_{2} = 0$$

$$\Delta^{2}\hat{\kappa}_{1} = 0.$$

Finally, for the precision of estimating ζ , we have

$$\begin{split} \delta\left(\frac{\zeta}{2}\right) &\geq \frac{1}{\sqrt{4\Delta^2\hat{\kappa}_3}} = \frac{1}{\sqrt{4\cdot6\Delta^2\hat{n}}} = \frac{1}{\sqrt{4\cdot9\cos^2\phi_2\Delta^2\hat{n}}} \\ \delta\zeta &\geq \frac{1}{3\sqrt{\cos^2\phi_2\Delta^2\hat{n}}}. \end{split}$$

Alternatively, we can estimate the parameter $\zeta \cos \phi_2 = (\theta_{2,3} + \theta_{1,3}) = \zeta \sqrt{\frac{2}{3}}$, for which the corresponding precision limit is given by:

$$\delta\left(\zeta\cos\phi_2\right) \ge \frac{1}{3\sqrt{\Delta^2\hat{n}}}.\tag{23}$$

This shows that, in practice, even though the phase reference mode is not directly measured and only the local variance is measured, the measured parameter $\theta_{1,3} + \theta_{2,3}$ is relative to the phase reference mode, making its presence essential.

Generalization to a k-mode state

We can generalize the above analysis to a (k+1)-mode state, where the (k+1)th mode serves as a phase reference for the remaining k modes. In this case, the state in eq. (11) generalizes to

$$|\psi\rangle = \sum_{\substack{n_1,\dots,n_k=0\\\sum_{m=1}^k n_m \le N}}^N c_{n_1\dots n_k} |n_1\rangle_1 \dots |n_k\rangle_k |N - \sum_m^k n_m\rangle_{k+1}.$$
(24)

In the (k+1)-mode case, the operator \hat{U} of eq. (12) extends to

$$\hat{U} = \prod_{\substack{i,j=1\\i>i}}^{k+1} e^{i\hat{J}_z^{(i,j)}\theta_{i,j}} = e^{i\sum_{i< j}^{k+1}\hat{J}_z^{(i,j)}\theta_{i,j}} = e^{\frac{i}{2}\sum_{i=1}^{k+1}\hat{n}_i\left(\sum_{j=i+1}^{k+1}\hat{n}_i\left(\sum_{j=i+1}^{k+1}\theta_{i,j}-\sum_{j=1}^{i-1}\theta_{j,i}\right)\right)}.$$
 (25)

Similar to the three-mode case discussed earlier, we can define transformations generated by the \hat{n}_m operators involving k+1 modes, analogous to the operators defined in eq. (13). To do so, we introduce a set of operators $\hat{\kappa}_{m,\phi}$, which depend on m independent parameters ϕ_m :

$$\hat{\kappa}_m = \sin \phi_m \hat{n}_{m+1} - \cos \phi_m \hat{\kappa}_{m-1,\phi_{m-1}}^{\perp},\tag{26}$$

with

$$\hat{\kappa}_{m}^{\perp} = \cos \phi_{m} \hat{n}_{m+1} + \sin \phi_{m} \hat{\kappa}_{m-1,\phi_{m-1}}^{\perp}, \tag{27}$$

where $m \in \{2, ..., k\}$. For m = 1 and m = k + 1 we define

$$\hat{\kappa}_1 = \sin \phi_1 \hat{n}_2 - \cos \phi_1 \hat{n}_1 \tag{28}$$

$$\hat{\vec{n}}_1^{\perp} = \sin \phi_1 \hat{n}_1 + \cos \phi_1 \hat{n}_2, \tag{29}$$

$$\hat{\kappa}_{k+1,\phi_k} = \hat{\kappa}_{k,\phi_k}^{\perp}.\tag{30}$$

With these definitions, the operators analogous to those in eq. (13) extend to dimension (k+1) as follows:

$$\hat{\kappa}_1 = \sin \phi_1 \hat{n}_2 - \cos \phi_1 \hat{n}_1 \tag{31a}$$

$$\hat{\kappa}_m = \sin \phi_m \hat{n}_{m+1} - \cos \phi_m \hat{\kappa}_{m-1,\phi_{m-1}}^{\perp}, \quad \text{for } m \in \{2, \dots, k\}$$
 (31b)

$$\hat{\vec{n}}_{k+1,\phi_k} = \hat{\kappa}_{k,\phi_k}^{\perp}. \tag{31c}$$

By expanding these operators in terms of the number operators \hat{n}_m , we obtain

$$\hat{\kappa}_1 = \sin \phi_1 \hat{n}_2 - \cos \phi_1 \hat{n}_1$$

 $\hat{\kappa}_2 = \sin \phi_2 \hat{n}_3 - \cos \phi_2 (\cos \phi_1 \hat{n}_2 + \sin \phi_1 \hat{n}_1) = \sin \phi_2 \hat{n}_3 - \cos \phi_2 \cos \phi_1 \hat{n}_2 - \cos \phi_2 \sin \phi_1 \hat{n}_1$

$$\hat{\kappa}_{m,\phi_m} = \sin \phi_m \hat{n}_{m+1} - \cos \phi_m \left(\cos \phi_{m-1} \hat{n}_m + \sum_{l=2}^{m-1} \left(\prod_{p=l}^{m-1} \sin \phi_p \right) \cos \phi_{l-1} \hat{n}_l + \left(\prod_{p=1}^{m-1} \sin \phi_p \right) \hat{n}_1 \right), \text{ for } m \in \{3, \dots, k\}$$

$$\hat{\kappa}_{k+1,\phi_k} = \cos\phi_k \hat{n}_{k+1} + \sin\phi_k \left(\cos\phi_{k-1}\hat{n}_k + \sum_{l=2}^{k-1} \left(\prod_{p=l}^{k-1} \sin\phi_p\right) \cos\phi_{l-1}\hat{n}_l + \left(\prod_{p=1}^{k-1} \sin\phi_p\right) \hat{n}_1\right)$$

$$(32)$$

$$= \cos \phi_k \hat{n}_{k+1} + \sum_{l=2}^k \left(\prod_{p=l}^k \sin \phi_p \right) \cos \phi_{l-1} \hat{n}_l + \left(\prod_{p=1}^k \sin \phi_p \right) \hat{n}_1$$

By estimating the variances of these operators, we can show that the following relation indeed holds:

$$\sum_{m=1}^{k} \Delta^2 \hat{\kappa}_{m,\phi_m} + \Delta^2 \hat{\kappa}_{k+1,\phi_k} = \sum_{m=1}^{k+1} \Delta^2 \hat{n}_m.$$
 (33)

By defining the parameters ζ and ϕ_i such that,

$$\zeta \hat{\kappa}_{k+1,\phi_k} = \sum_{i=1}^{k+1} \hat{n}_i \left(\sum_{j=i+1}^{k+1} \theta_{i,j} - \sum_{j=1}^{i-1} \theta_{j,i} \right)$$
(34)

the operator in eq. (25) becomes

$$\prod_{\substack{i,j=1\\j>i}}^{k+1} e^{i\hat{J}_z^{(i,j)}\theta_{i,j}} = e^{i\frac{\zeta}{2}\hat{\kappa}_{k+1,\phi_k}}.$$
(35)

From the equality in eq. (34), and using the expansion of $\hat{\kappa}_{k+1,\phi_k}$ derived in (32), we can identify the parameters ζ and ϕ_k as follows:

$$\zeta \cos \phi_k = -\sum_{j=1}^k \theta_{j,k+1}$$

$$\zeta \left(\prod_{p=1}^k \sin \phi_p \right) \cos \phi_{i-1} = \sum_{j=i+1}^{k+1} \theta_{i,j} - \sum_{j=1}^{i-1} \theta_{j,i}, \quad \text{for } i = 2, \dots, k$$

$$\prod_{p=1}^k \sin \phi_p = \sum_{j=2}^{k+1} \theta_{1,j}.$$

By maximizing the variance $\Delta^2 \hat{\kappa}_{k+1,\phi_k}$, we achieve the highest precision in estimating the parameter ζ . According to relation (33), the maximum of $\Delta^2 \hat{\kappa}_{k+1,\phi_k}$ is bounded by $\sum_{m=1}^{k+1} \Delta^2 \hat{n}_m$, and this bound is reached when $\sum_{m=1}^k \Delta^2 \hat{\kappa}_{m,\phi_m} = 0$. Additionally, using the fact that $n_{k+1} = N - \sum_{m=1}^k n_m$, we have

$$\Delta^{2} \hat{n}_{k+1} = \sum_{\substack{n_{1}, \dots, n_{k} = 0 \\ \sum_{m=1}^{k} n_{m} \leq N}}^{N} |c_{n_{1} \dots n_{k}}|^{2} \left(N - \sum_{m=1}^{k} n_{m}\right)^{2} - \left(\sum_{\substack{n_{1}, \dots, n_{k} = 0 \\ \sum_{m=1}^{k} n_{m} \leq N}}^{N} |c_{n_{1} \dots n_{k}}|^{2} \left(N - \sum_{m=1}^{k} n_{m}\right)^{2} - \left(\sum_{m=1}^{k} \overline{n}_{m} \leq N\right)^{2}$$

$$= \sum_{\substack{n_{1}, \dots, n_{k} = 0 \\ \sum_{m=1}^{k} n_{m} \leq N}}^{N} |c_{n_{1} \dots n_{k}}|^{2} \left(\sum_{m=1}^{k} n_{m}\right)^{2} - \left(\sum_{m=1}^{k} \overline{n}_{m}\right)^{2}$$

$$= \sum_{m=1}^{k} \Delta^{2} \hat{n}_{m} + 2 \sum_{m=1}^{k-1} \sum_{n>m}^{k} \operatorname{Cov}\{\hat{n}_{m}, \hat{n}_{p}\} = \Delta^{2} \hat{n}_{col}, \tag{36}$$

where we define collective photon number operator

$$\hat{n}_{\text{col}} = \sum_{m=1}^{k} \hat{n}_m,\tag{37}$$

which represents the total number of photons occupying the first k modes. Taking into account this relation, eq. (33) becomes

$$\sum_{m=1}^{k} \Delta^2 \hat{\kappa}_{m,\phi_m} + \Delta^2 \hat{\kappa}_{k+1,\phi_k} = 2 \sum_{m=1}^{k} \Delta^2 \hat{n}_m + 2 \sum_{m=1}^{k-1} \sum_{p>m}^{k} \text{Cov}\{\hat{n}_m, \hat{n}_p\} = \sum_{m=1}^{k} \Delta^2 \hat{n}_m + \Delta^2 \hat{n}_{\text{col}}.$$

Thus, the precision limit for estimating ζ , which is achieved by maximizing $\Delta^2 \hat{\kappa}_{k+1,\phi_k}$, is given by

$$\delta\zeta \ge \frac{1}{\sqrt{2\sum_{m=1}^{k} \Delta^2 \hat{n}_m + 2\sum_{m=1}^{k-1} \sum_{p>m}^{k} \text{Cov}\{\hat{n}_m, \hat{n}_p\}}} = \frac{1}{\sqrt{\sum_{m=1}^{k} \Delta^2 \hat{n}_m + \Delta^2 \hat{n}_{\text{col}}}}.$$
 (38)

This expression generalizes the bound given in eq. (20) and explicitly shows that the precision limit depends not only on the total number of photons present in the system of interest (i.e., in the first k modes, excluding the phase reference), but also on how those photons are distributed across the k modes.

As an example, we consider a specific state in which there are no correlations between photons in different modes m, i.e., $\text{Cov}\{\hat{n}_m, \hat{n}_p\} = 0$, $m, p \leq k$. In this case, the precision bound becomes

$$\delta\zeta \ge \frac{1}{\sqrt{2\sum_{m=1}^{k} \Delta^2 \hat{n}_m}}.$$
(39)

Since there are no correlations between the modes, we have $\Delta^2 \hat{n}_{\text{col}} = \sum_{m=1}^k \Delta^2 \hat{n}_m$. This shows that, for such a state, the precision scales with the collective number—that is, the total number of photons in the first k modes. Thus,

this state can be regarded as equivalent to a two-mode state, where $\sum_{m=1}^k n_m$ uncorrelated photons occupy the first mode, and $N - \sum_{m=1}^k n_m$ photons occupy the second (reference) mode. In this case, the precision of estimation depends only on the total number of photons, not on the number of modes. In particular, if the state satisfies $\Delta^2 \hat{n}_1 = \Delta^2 \hat{n}_2 = \cdots = \Delta^2 \hat{n}_k = \Delta^2 \hat{n}$, then

$$\delta\zeta \ge \frac{1}{\sqrt{2k\Delta^2\hat{n}}},\tag{40}$$

i.e., the quantum Fisher information (QFI) scales at most linearly with the number of modes.

We now consider a case with highly correlated photons, where each of the first k modes contains the same number of photons: $n_1 = n_2 = \cdots = n_k = n$, and the (k+1)th mode contains $n_{k+1} = N - kn$ photons. In this case the covariance between any two distinct modes is

$$\operatorname{Cov}\{\hat{n}_m, \hat{n}_p\} = \Delta^2 \hat{n}$$

for $m, p \leq k$ and the total variance becomes

$$\sum_{m=1}^{k} \Delta^{2} \hat{\kappa}_{m,\phi_{m}} + \Delta^{2} \hat{\kappa}_{k+1,\phi_{k}} = 2k\Delta^{2} \hat{n} + 2\frac{k(k-1)}{2} \Delta^{2} \hat{n} = k(k+1)\Delta^{2} \hat{n}$$
(41)

$$= \Delta^2 (k\hat{n}) + k\Delta^2 \hat{n} = \Delta^2 \hat{n}_{\text{col}} + k\Delta^2 \hat{n}. \tag{42}$$

Thus, the precision limit when maximizing $\Delta^2 \hat{\kappa}_{k+1,\phi_k}$ (i.e., when $\sum_{m=1}^k \Delta^2 \hat{\kappa}_{m,\phi_m} = 0$) becomes

$$\delta\zeta \ge \frac{1}{\sqrt{\Delta^2 \hat{n}_{\text{col}} + k\Delta^2 \hat{n}}} = \frac{1}{\sqrt{k(k+1)\Delta^2 \hat{n}}} \tag{43}$$

Comparing this with the case discussed in eq. (40), we see that for such a highly correlated state, the precision scales quadratically with the number of modes. This quadratic scaling arises from estimating the correlations between the modes, given by: $2\sum_{m=1}^{k-1}\sum_{p>m}^{k}\operatorname{Cov}\{\hat{n}_{m},\hat{n}_{p}\}.$

As mentioned earlier, to maximize $\Delta^2 \hat{\kappa}_{k+1,\phi_k}$, we impose the condition

$$\sum_{m=1}^{k} \Delta^2 \hat{\kappa}_{m,\phi_m} = 0. \tag{44}$$

Below we determine the parameters ϕ_m that satisfy this condition. We begin by noting that, for a state with an equal number of photons in each mode, while the operators \hat{n}_m are different, their action on the state is the same for all $m \in \{1, \dots k\}$, thus in the expressions in eq. (32) we factor these operators by denoting $\hat{n}_1 = \dots = \hat{n}_k = \hat{n}$ and the expressions simplify to:

$$\hat{\kappa}_{1} = (\sin \phi_{1} - \cos \phi_{1}) \,\hat{n}$$

$$\hat{\kappa}_{2} = (\sin \phi_{2} - \cos \phi_{2} (\cos \phi_{1} + \sin \phi_{1})) \,\hat{n}$$

$$\hat{\kappa}_{m,\phi_{m}} = \left(\sin \phi_{m} - \cos \phi_{m} \left(\cos \phi_{m-1} + \sum_{l=2}^{m-1} \left(\prod_{p=l}^{m-1} \sin \phi_{p}\right) \cos \phi_{l-1} + \prod_{p=1}^{m-1} \sin \phi_{p}\right)\right) \,\hat{n}, \text{ for } m = \{3, \dots, k-1\}$$

$$\hat{\kappa}_{k,\phi_{k}} = \sin \phi_{k} (N - k\hat{n}) - \cos \phi_{k} \left(\cos \phi_{k-1} + \sum_{l=2}^{k-1} \left(\prod_{p=l}^{k-1} \sin \phi_{p}\right) \cos \phi_{l-1} + \prod_{p=1}^{k-1} \sin \phi_{p}\right) \hat{n},$$

$$\hat{\kappa}_{k+1,\phi_{k}} = \cos \phi_{k} (N - k\hat{n}) + \left(\sum_{l=2}^{k} \left(\prod_{p=l}^{k} \sin \phi_{p}\right) \cos \phi_{l-1} + \prod_{p=1}^{k} \sin \phi_{p}\right) \hat{n},$$
(45)

where we have also used the fact that $\hat{n}_{k+1} = N - k\hat{n}$. Using these expressions, we find that the condition in eq. (44)

is satisfied by choosing the parameters ϕ_m such that

$$\sin \phi_1 = \cos \phi_1 = \frac{1}{\sqrt{2}}$$

$$\sin \phi_2 = \cos \phi_2 (\cos \phi_1 + \sin \phi_1) = \sqrt{2} \cos \phi_2 = \sqrt{\frac{2}{3}}$$

$$\sin \phi_m = \cos \phi_m \sqrt{m} = \sqrt{\frac{m}{m+1}}, \quad \text{for } m = 3, \dots, k-1.$$

With these choices, all variances $\Delta^2 \hat{\kappa}_{m,\phi_m}$ for $m = \{1,\ldots,k-1\}$ vanish. For m = k we have:

$$\hat{\kappa}_{k,\phi_k} = \sin \phi_k \left(N - k\hat{n} \right) - \cos \phi_k \sqrt{k} \hat{n} = \sin \phi_k N - \left(k \sin \phi_k + \cos \phi_k \sqrt{k} \right) \hat{n}.$$

Requiring the variance $\Delta^2 \hat{\kappa}_{k,\phi_k}$ to vanish implies:

$$\sin \phi_k = -\frac{1}{\sqrt{k}} \cos \phi_k = \frac{1}{\sqrt{k+1}}.\tag{46}$$

With this value of ϕ_k , the operator $\hat{\kappa}_{k+1,\phi_k}$ becomes:

$$\hat{\kappa}_{k+1,\phi_k} = \cos\phi_k \left(N - k\hat{n}\right) + \sin\phi_k \sqrt{k}\hat{n} = \cos\phi_k \left(N - k\hat{n}\right) - \cos\phi_k \hat{n} = \cos\phi_k \left(N - (k+1)\hat{n}\right),\tag{47}$$

and the variance is:

$$\Delta^{2}\hat{\kappa}_{k+1,\phi_{k}} = \cos^{2}\phi_{k}(k+1)^{2}\Delta^{2}\hat{n} = \frac{k}{k+1}(k+1)^{2}\Delta^{2}\hat{n} = k(k+1)\Delta^{2}\hat{n},\tag{48}$$

which indeed recovers the maximum variance given in (41). The corresponding precision limit for estimating ζ is then:

$$\zeta \ge \frac{1}{\sqrt{(k+1)^2 \cos^2 \phi_k \Delta^2 \hat{n}}} = \frac{1}{\sqrt{k(k+1)\Delta^2 \hat{n}}}.$$
 (49)

If instead we estimate the parameter $\zeta \cos \phi_k = -\sum_{j=1}^k \theta_{j,k+1}$, the bound becomes:

$$\zeta \cos \phi_k \ge \frac{1}{\sqrt{(k+1)^2 \Delta^2 \hat{n}}}.$$
(50)

That is, the QFI for estimating the collective parameter $\sum_{j=1}^{k} \theta_{j,k+1}$ scales quadratically with the number of modes, including the phase reference mode. This illustrates how entanglement "replaces" coherence in scaling, and identifies the origin of quadratic scaling for entangled states with fixed total photon number but with a rich entangled modal structure as we will see in the following illustrative example.

Application: correlation between internal degrees of freedom of single photons

We now use the previous results to analyze the problem of parameter estimation using states with both an external mode structure (as the ket's subscripts in the previous section) and an internal mode structure, as temporal and frequency modes. For instance, a single photon state that propagates in mode 1 with a spectral amplitude $f(\omega)$ can be written as $|\psi\rangle = \left(\int f(\omega) \hat{a}_1^{\dagger}(\omega) d\omega\right) |\emptyset\rangle = \int f(\omega) |\omega\rangle_1 d\omega$. Of course, different states can be considered, with many propagation modes (external modes) and frequency modes (internal modes) that can be correlated or separable. We will study the case of multiple single photon states where each photon occupies a single propagation mode and the frequency modes can be entangled or separable, as in [9, 10], for instance, or in [46, 102–104] on its two-photon version. A general k photon state can thus be written as

$$\int d\omega_1...\omega_k f(\omega_1,...,\omega_k) |\omega_1,...,\omega_k\rangle.$$

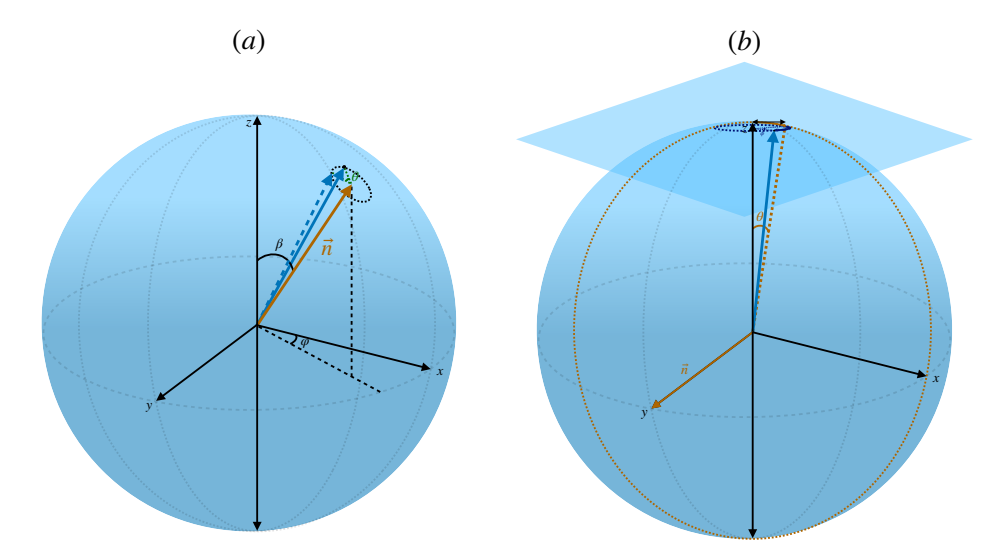


FIG. 1: (a) Rotation of the original state (dashed blue line) by an angle θ around the axis $\hat{\vec{n}}$, defined by polar angle β and azimuthal angle φ . (b) Rotation of the state (blue line) around the y-axis by a small angle θ , followed by a rotation around the z-axis by an angle φ . For such a small angle θ , this transformation corresponds to a displacement on the tangent plane.

In this context, we can model the evolution by replacing $\theta_{i,j}\hat{J}_{\vec{n}}^{(i,j)}\to t\int\omega\hat{J}_{\vec{n}}^{(i,j)}(\omega)d\omega$, where t has dimension of time. It is then possible to perform the same analysis that has been done for \hat{n}_i in Eqs. (31) with operators $\int\omega\hat{n}_i(\omega)d\omega=\hat{\omega}_i$, and the parameter to be estimated is now t. If we now inspect Eqs. (40) and (50) and consider the estimation of t, we must replace $\Delta^2\hat{n}_i\to\Delta^2\hat{\omega}_i$. Notice that $\Delta^2\hat{\omega}_i=\left(\int\prod_{j=1}^kd\omega_j|f(\omega_1,...,\omega_i,...\omega_k)|^2\omega_i^2\right)-\left(\int\prod_{j=1}^kd\omega_j|f(\omega_1,...,\omega_i,...\omega_k)|^2\omega_i\right)^2$ in this case, and we can consider for simplicity that $\Delta^2\hat{\omega}_i=\Delta^2\hat{\omega}~\forall~i$. Hence, Eqs. (40) and (50) lead to the same scaling found in [10] and [9] for, respectively, separable states with an internal mode structure and entangled states where internal and external degrees of freedom are maximally correlated, using a different and more general approach.

Parameter Estimation with an Arbitrary Generator on a Multimode State in the CV limit

We extend the above analysis to a general case where the transformation is performed using a collective operator associated with a rotations around the arbitrary direction $\vec{n} = \{\cos\varphi\sin\beta, \sin\varphi\sin\beta, \cos\beta\}$ with small angles $\theta_{i,j}/\sqrt{N}$, such that $\theta_{i,j}^2/N \ll 1$ (see Fig. 1). For a three-mode system, the total unitary can be written as a product of two-mode rotations:

$$\prod_{i < j = 1}^{3} e^{i\hat{J}_{\vec{n}}^{(i,j)} \frac{\theta_{i,j}}{\sqrt{N}}} = e^{i\hat{J}_{\vec{n}}^{(2,3)} \frac{\theta_{2,3}}{\sqrt{N}}} e^{i\hat{J}_{\vec{n}}^{(1,3)} \frac{\theta_{1,3}}{\sqrt{N}}} e^{i\hat{J}_{\vec{n}}^{(1,2)} \frac{\theta_{1,2}}{\sqrt{N}}} \approx e^{\frac{i}{\sqrt{N}} \left(\hat{J}_{\vec{n}}^{(1,2)} \theta_{1,2} + \hat{J}_{\vec{n}}^{(1,3)} \theta_{1,3} + \hat{J}_{\vec{n}}^{(2,3)} \theta_{2,3}\right)},$$
(51)

where the final expression is obtained taking into account the fact that $\frac{\theta_{i,j}\theta_{i',j'}}{N}\left[\hat{J}_{\vec{n}}^{(i,j)},\hat{J}_{\vec{n}}^{(i',j')}\right] \ll 1$. We then introduce transformations generated by operators $\hat{\kappa}_m$ analogous to the ones defined in (13) with

$$\hat{\kappa}_3 = \cos\phi_2 \hat{J}_{\vec{n}}^{(1,2)} + \sin\phi_2 \left(\cos\phi_1 \hat{J}_{\vec{n}}^{(1,3)} + \sin\phi_1 \hat{J}_{\vec{n}}^{(2,3)}\right),\tag{52a}$$

$$\hat{\kappa}_2 = \sin \phi_2 \hat{J}_{\vec{n}}^{(1,2)} - \cos \phi_2 \left(\cos \phi_1 \hat{J}_{\vec{n}}^{(1,3)} + \sin \phi_1 \hat{J}_{\vec{n}}^{(2,3)} \right), \tag{52b}$$

$$\hat{\kappa}_1 = \sin \phi_1 \hat{J}_{\vec{n}}^{(1,3)} - \cos \phi_1 \hat{J}_{\vec{n}}^{(2,3)}. \tag{52c}$$

We next define the parameters χ and ϕ_m via the following relations:

$$\chi \cos \phi_2 = 2\theta_{1,2},\tag{53a}$$

$$\chi \sin \phi_2 \cos \phi_1 = 2\theta_{1.3},\tag{53b}$$

$$\chi \sin \phi_2 \sin \phi_1 = 2\theta_{2,3},\tag{53c}$$

which leads to $\chi^2 = 4 \left(\theta_{1,2}^2 + \theta_{1,3}^2 + \theta_{2,3}^2\right)$. With these definitions, the operator in (51) can be written as

$$e^{\frac{i}{\sqrt{N}} \left(\hat{J}_{\vec{n}}^{(1,2)} \theta_{1,2} + \hat{J}_{\vec{n}}^{(1,3)} \theta_{1,3} + \hat{J}_{\vec{n}}^{(2,3)} \theta_{2,3} \right)} = e^{i \frac{\chi}{2\sqrt{N}} \hat{\kappa}_3}. \tag{54}$$

Thus, the effective generator of the collective transformation is given by $\hat{\kappa}_3$. By computing the variances of the operators in eq. (52), we obtain the following expressions:

$$\begin{split} \Delta^2 \hat{\kappa}_3 &= \cos^2 \phi_2 \Delta^2 \hat{J}_{\vec{n}}^{(1,2)} + \sin^2 \phi_2 \cos^2 \phi_1 \Delta^2 \hat{J}_{\vec{n}}^{(1,3)} + \sin^2 \phi_2 \sin^2 \phi_1 \Delta^2 \hat{J}_{\vec{n}}^{(2,3)} \\ &+ \sin \phi_2 \cos \phi_2 \Bigg(\cos \phi_1 \left(\text{Cov} \{ \hat{J}_{\vec{n}}^{(1,3)}, \hat{J}_{\vec{n}}^{(1,2)} \} + \text{Cov} \{ \hat{J}_{\vec{n}}^{(1,2)}, \hat{J}_{\vec{n}}^{(1,3)} \} \Big) \\ &+ \sin \phi_1 \left(\text{Cov} \{ \hat{J}_{\vec{n}}^{(2,3)}, \hat{J}_{\vec{n}}^{(1,2)} \} + \text{Cov} \{ \hat{J}_{\vec{n}}^{(1,2)}, \hat{J}_{\vec{n}}^{(2,3)} \} \right) \Bigg) \\ &+ \sin^2 \phi_2 \cos \phi_1 \sin \phi_1 \left(\text{Cov} \{ \hat{J}_{\vec{n}}^{(1,3)}, \hat{J}_{\vec{n}}^{(2,3)} \} + \text{Cov} \{ \hat{J}_{\vec{n}}^{(2,3)}, \hat{J}_{\vec{n}}^{(1,3)} \} \right) \\ \Delta^2 \hat{\kappa}_2 &= \sin^2 \phi_2 \Delta^2 \hat{J}_{\vec{n}}^{(1,2)} + \cos^2 \phi_2 \cos^2 \phi_1 \Delta^2 \hat{J}_{\vec{n}}^{(1,3)} + \cos^2 \phi_2 \sin^2 \phi_1 \Delta^2 \hat{J}_{\vec{n}}^{(2,3)} \\ &- \sin \phi_2 \cos \phi_2 \Bigg(\cos \phi_1 \left(\text{Cov} \{ \hat{J}_{\vec{n}}^{(1,3)}, \hat{J}_{\vec{n}}^{(1,2)} \} + \text{Cov} \{ \hat{J}_{\vec{n}}^{(1,2)}, \hat{J}_{\vec{n}}^{(1,3)} \} \right) \\ &+ \sin \phi_1 \left(\text{Cov} \{ \hat{J}_{\vec{n}}^{(2,3)}, \hat{J}_{\vec{n}}^{(1,2)} \} + \text{Cov} \{ \hat{J}_{\vec{n}}^{(1,2)}, \hat{J}_{\vec{n}}^{(2,3)} \} \right) \Bigg) \\ &+ \cos^2 \phi_2 \cos \phi_1 \sin \phi_1 \left(\text{Cov} \{ \hat{J}_{\vec{n}}^{(1,3)}, \hat{J}_{\vec{n}}^{(2,3)} \} + \text{Cov} \{ \hat{J}_{\vec{n}}^{(2,3)}, \hat{J}_{\vec{n}}^{(1,3)} \} \right) \\ \Delta^2 \hat{\kappa}_1 &= \sin^2 \phi_1 \Delta^2 \hat{J}_{\vec{n}}^{(1,3)} + \cos^2 \phi_1 \Delta^2 \hat{J}_{\vec{n}}^{(2,3)} - \sin \phi_1 \cos \phi_1 \left(\text{Cov} \{ \hat{J}_{\vec{n}}^{(1,3)}, \hat{J}_{\vec{n}}^{(2,3)} \} + \text{Cov} \{ \hat{J}_{\vec{n}}^{(1,3)}, \hat{J}_{\vec{n}}^{(2,3)} \} \right) \Bigg) \\ \Delta^2 \hat{\kappa}_1 &= \sin^2 \phi_1 \Delta^2 \hat{J}_{\vec{n}}^{(1,3)} + \cos^2 \phi_1 \Delta^2 \hat{J}_{\vec{n}}^{(2,3)} - \sin \phi_1 \cos \phi_1 \left(\text{Cov} \{ \hat{J}_{\vec{n}}^{(1,3)}, \hat{J}_{\vec{n}}^{(2,3)} \} + \text{Cov} \{ \hat{J}_{\vec{n}}^{(1,3)}, \hat{J}_{\vec{n}}^{(2,3)} \} \right) \Bigg) \\ \Delta^2 \hat{\kappa}_1 &= \sin^2 \phi_1 \Delta^2 \hat{J}_{\vec{n}}^{(1,3)} + \cos^2 \phi_1 \Delta^2 \hat{J}_{\vec{n}}^{(2,3)} - \sin \phi_1 \cos \phi_1 \left(\text{Cov} \{ \hat{J}_{\vec{n}}^{(1,3)}, \hat{J}_{\vec{n}}^{(2,3)} \} + \text{Cov} \{ \hat{J}_{\vec{n}}^{(1,3)}, \hat{J}_{\vec{n}}^{(2,3)} \} \right) \Bigg) \\ \hat{\kappa}_1 &= \sin^2 \phi_1 \Delta^2 \hat{J}_{\vec{n}}^{(1,3)} + \cos^2 \phi_1 \Delta^2 \hat{J}_{\vec{n}}^{(2,3)} - \sin \phi_1 \cos \phi_1 \left(\text{Cov} \{ \hat{J}_{\vec{n}}^{(1,3)}, \hat{J}_{\vec{n}}^{(2,3)} \} \right) \Bigg) \Bigg) \\ \hat{\kappa}_2 &= \sin^2 \phi_1 \Delta^2 \hat{J}_{\vec{n}}^{(1,3)} + \cos^2 \phi_1 \Delta^2 \hat{J}_{\vec{n}}^{(2,3)} - \sin \phi_1 \cos \phi_1 \left(\text{Cov} \{ \hat{J}_{\vec{n}}^{(1,3)}, \hat{J}_{\vec{n}}^{(2,3)} \} \right) \Bigg) \Bigg)$$

We can now observe that the sum of the variances of the three collective operators is equal to the sum of the local variances:

$$\Delta^2 \hat{\kappa}_1 + \Delta^2 \hat{\kappa}_2 + \Delta^2 \hat{\kappa}_3 = \Delta^2 \hat{J}_{\vec{n}}^{(1,2)} + \Delta^2 \hat{J}_{\vec{n}}^{(1,3)} + \Delta^2 \hat{J}_{\vec{n}}^{(2,3)}. \tag{55}$$

Hence, the total variance is conserved and maximizing $\Delta^2 \hat{\kappa}_3$ (and the QFI for χ) is equivalent to minimizing the variances of $\hat{\kappa}_2$ and $\hat{\kappa}_2$.

To estimate these variances, we recall that each $\Delta^2 \hat{J}_{\vec{n}}^{(i,j)}$ can be expanded in terms of the x,y,z components of the angular momentum operators:

$$\begin{split} \Delta^2 \hat{J}_{\vec{n}}^{(i,j)} &= \Delta^2 \hat{J}_x^{(i,j)} \cos^2 \varphi \sin^2 \beta + \Delta^2 \hat{J}_y^{(i,j)} \sin^2 \varphi \sin^2 \beta + \Delta^2 \hat{J}_z^{(i,j)} \cos^2 \beta \\ &\quad + \left(\operatorname{Cov} \{ \hat{J}_x^{(i,j)}, \hat{J}_y^{(i,j)} \} + \operatorname{Cov} \{ \hat{J}_y^{(i,j)}, \hat{J}_x^{(i,j)} \} \right) \cos \varphi \sin \varphi \sin^2 \beta \\ &\quad + \left(\operatorname{Cov} \{ \hat{J}_x^{(i,j)}, \hat{J}_z^{(i,j)} \} + \operatorname{Cov} \{ \hat{J}_z^{(i,j)}, \hat{J}_x^{(i,j)} \} \right) \cos \varphi \sin \beta \cos \beta \\ &\quad + \left(\operatorname{Cov} \{ \hat{J}_y^{(i,j)}, \hat{J}_z^{(i,j)} \} + \operatorname{Cov} \{ \hat{J}_z^{(i,j)}, \hat{J}_y^{(i,j)} \} \right) \sin \varphi \sin \beta \cos \beta. \end{split}$$

Summing over all pairs (i < j) gives:

$$\begin{split} \sum_{i < j}^{3} \Delta^{2} \hat{J}_{\vec{n}}^{(i,j)} &= \sum_{i < j}^{3} \Delta^{2} \hat{J}_{x}^{(i,j)} \cos^{2} \varphi \sin^{2} \beta + \sum_{i < j}^{3} \Delta^{2} \hat{J}_{y}^{(i,j)} \sin^{2} \varphi \sin^{2} \beta + \sum_{i < j}^{3} \Delta^{2} \hat{J}_{z}^{(i,j)} \cos^{2} \beta \\ &+ \sum_{i < j}^{3} \left(\operatorname{Cov} \{ \hat{J}_{x}^{(i,j)}, \hat{J}_{y}^{(i,j)} \} + \operatorname{Cov} \{ \hat{J}_{y}^{(i,j)}, \hat{J}_{x}^{(i,j)} \} \right) \cos \varphi \sin \varphi \sin^{2} \beta \\ &+ \sum_{i < j}^{3} \left(\operatorname{Cov} \{ \hat{J}_{x}^{(i,j)}, \hat{J}_{z}^{(i,j)} \} + \operatorname{Cov} \{ \hat{J}_{z}^{(i,j)}, \hat{J}_{x}^{(i,j)} \} \right) \cos \varphi \sin \beta \cos \beta \\ &+ \sum_{i < j}^{3} \left(\operatorname{Cov} \{ \hat{J}_{y}^{(i,j)}, \hat{J}_{z}^{(i,j)} \} + \operatorname{Cov} \{ \hat{J}_{z}^{(i,j)}, \hat{J}_{y}^{(i,j)} \} \right) \sin \varphi \sin \beta \cos \beta. \end{split}$$

We can now examine the limit $N \to \infty$, in which mode 3 acts as a classical reference. In this regime, with modes 1 and 2 having finite number of photons, the two-mode coupling operators become continuous-variable quadratures. To demonstrate this, without loss of generality, we consider a particular case where $\hat{J}_{\vec{n}} = \hat{J}_y$, i.e., $\beta = \pi/2$, $\varphi = \pi/2$. In this case, the bound for the sum of the variances in (55) becomes $\Delta^2 \hat{J}_y^{(1,2)} + \Delta^2 \hat{J}_y^{(1,3)} + \Delta^2 \hat{J}_y^{(2,3)}$. To compute these variances we first note that for a general k-mode state

$$|\psi\rangle = \sum_{n_1 \cdots n_k} c_{n_1, \cdots, n_k} |n_1\rangle_1 |n_2\rangle_2 \cdots |n_k\rangle_k,$$

with $\sum_{i=1}^{k} n_i = N$, the variance of $\hat{J}_y^{(i,j)}$ for any two modes i, j is

$$\Delta^2 \hat{J}_y^{(i,j)} = \langle \left(\hat{J}_y^{(i,j)} \right)^2 \rangle - \langle \hat{J}_y^{(i,j)} \rangle,$$

with

$$\begin{split} \langle \left(\hat{J}_{y}^{(i,j)} \right)^{2} \rangle &= -\frac{1}{4} \langle \psi | \left(\hat{a}_{i} \hat{a}_{j}^{\dagger} \hat{a}_{i} \hat{a}_{j}^{\dagger} - \hat{a}_{i} \hat{a}_{j}^{\dagger} \hat{a}_{i}^{\dagger} \hat{a}_{j} - \hat{a}_{i}^{\dagger} \hat{a}_{j} \hat{a}_{i} \hat{a}_{j}^{\dagger} + \hat{a}_{i}^{\dagger} \hat{a}_{j} \hat{a}_{i}^{\dagger} \hat{a}_{j} \right) | \psi \rangle \\ &= -\frac{1}{4} \sum_{n_{1} \cdots n_{k}} \left(c_{n_{1}, \cdots, n_{i}-2, \cdots, n_{j}+2, \cdots, n_{k}}^{*} c_{n_{1}, \cdots, n_{k}} \sqrt{n_{i} \left(n_{i}-1 \right) \left(n_{j}+1 \right) \left(n_{j}+2 \right)} \right. \\ &+ c_{n_{1}, \cdots, n_{i}+2, \cdots, n_{j}-2, \cdots, n_{k}}^{*} c_{n_{1}, \cdots, n_{k}} \sqrt{n_{j} \left(n_{j}-1 \right) \left(n_{i}+1 \right) \left(n_{i}+2 \right)} \right) \\ &+ \frac{1}{4} \sum_{n_{1} \cdots n_{k}} |c_{n_{1}, \cdots, n_{k}}|^{2} \left(n_{j} \left(n_{i}+1 \right) + n_{i} \left(n_{j}+1 \right) \right), \\ \langle \left(\hat{J}_{y}^{(i,j)} \right) \rangle &= \frac{i}{2} \langle \left(\hat{a}_{i} \hat{a}_{j}^{\dagger} - \hat{a}_{i}^{\dagger} \hat{a}_{j} \right) \rangle \\ &= \frac{i}{2} \sum_{n_{1} \cdots n_{k}} \left(c_{n_{1}, \cdots, n_{i}-1, \cdots, n_{j}+1, \cdots, n_{k}}^{*} c_{n_{1}, \cdots, n_{k}} \sqrt{n_{i} \left(n_{j}+1 \right) - c_{n_{1}, \cdots, n_{i}+1, \cdots, n_{j}-1, \cdots, n_{k}}^{*} c_{n_{1}, \cdots, n_{k}} \sqrt{n_{j} \left(n_{i}+1 \right)} \right). \end{split}$$

For the three-mode case, whenever the rotation involves one of the first two modes and the third (reference) mode,

we can analyze the limit $N \to \infty$:

$$\begin{split} \langle \left(\hat{J}_{y}^{(1,3)} \right)^{2} \rangle &= -\frac{1}{4} \sum_{n_{1},n_{2}} \left(c_{n_{1}-2,n_{2}}^{*} c_{n_{1},n_{2}} \sqrt{n_{1} \left(n_{1}-1 \right) \left(N-\left(n_{1}+n_{2} \right) +1 \right) \left(N-\left(n_{1}+n_{2} \right) +2 \right)} \right. \\ &+ c_{n_{1}+2,n_{2}}^{*} c_{n_{1},n_{2}} \sqrt{\left(N-\left(n_{1}+n_{2} \right) \right) \left(N-\left(n_{1}+n_{2} \right) -1 \right) \left(n_{1}+1 \right) \left(n_{1}+2 \right)} \right) \\ &+ \frac{1}{4} \sum_{n_{1},n_{2}} \left| c_{n_{1},n_{2}} \right|^{2} \left(\left(N-\left(n_{1}+n_{2} \right) \right) \left(n_{1}+1 \right) +n_{1} \left(N-\left(n_{1}+n_{2} \right) +1 \right) \right) \\ &+ \frac{N}{4} \sum_{n_{1},n_{2}} \left| c_{n_{1},n_{2}} c_{n_{1},n_{2}} \sqrt{n_{1} \left(n_{1}-1 \right)} + c_{n_{1}+2,n_{2}}^{*} c_{n_{1},n_{2}} \sqrt{\left(n_{1}+1 \right) \left(n_{1}+2 \right)} \right) \\ &+ \frac{N}{4} \sum_{n_{1},n_{2}} \left| c_{n_{1},n_{2}} \right|^{2} \left(2n_{1}+1 \right) = N \langle \left(\frac{i}{2} \left(\hat{a}_{1} - \hat{a}_{1}^{\dagger} \right) \right)^{2} \rangle = N \langle \hat{p}_{1}^{2} \rangle \\ &\langle \left(\hat{J}_{y}^{(1,3)} \right) \rangle = \frac{i}{2} \sum_{n_{1},n_{2}} \left(c_{n_{1}-1,n_{2}}^{*} c_{n_{1},n_{2}} \sqrt{n_{1} \left(N-\left(n_{1}+n_{2} \right) +1 \right)} - c_{n_{1}+1,n_{2}}^{*} c_{n_{1},n_{2}} \sqrt{\left(N-\left(n_{1}+n_{2} \right) \right) \left(n_{1}+1 \right)} \right) \\ &+ \sum_{N \to \infty} \frac{i}{2} \sqrt{N} \sum_{n_{1},n_{2}} \left(c_{n_{1}-1,n_{2}}^{*} c_{n_{1},n_{2}} \sqrt{n_{1}} - c_{n_{1}+1,n_{2}}^{*} c_{n_{1},n_{2}} \sqrt{\left(n_{1}+1 \right)} \right) = \sqrt{N} \langle \frac{i}{2} \left(\hat{a}_{1} - \hat{a}_{1}^{\dagger} \right) \rangle = \sqrt{N} \langle \hat{p}_{1} \rangle, \end{split}$$

where we have defined the quadrature operator $\hat{p}_1 = \frac{i}{2} \left(\hat{a}_1 - \hat{a}_1^{\dagger} \right)$, that acts on the approximated state

$$|\psi\rangle \underset{N\to\infty}{\approx} \sum_{\substack{n_1,n_2=0\\n_1+n_2\leqslant N}}^{N} c_{n_1,n_2}|n_1\rangle_1|n_2\rangle_2|N\rangle_3.$$

Hence:

$$\Delta^2 \hat{J}_y^{(1,3)} = N \Delta^2 \hat{p}_1.$$

Similarly, we can show that

$$\Delta^2 \hat{J}_y^{(2,3)} = N \Delta^2 \hat{p}_2,$$

with $\hat{p}_2 = \frac{i}{2} \left(\hat{a}_2 - \hat{a}_2^{\dagger} \right)$. To estimate $\Delta^2 \hat{J}_y^{(1,2)}$, we have that

$$\begin{split} \langle \left(\hat{J}_{y}^{(1,2)} \right)^{2} \rangle &= -\frac{1}{4} \langle \left(\hat{a}_{1} \hat{a}_{2}^{\dagger} - \hat{a}_{1}^{\dagger} \hat{a}_{2} \right)^{2} \rangle \\ &= -\frac{1}{4} \sum_{n_{1},n_{2}} \left(c_{n_{1}-2,n_{2}+2}^{*} c_{n_{1},n_{2}} \sqrt{n_{1} \left(n_{1}-1 \right) \left(n_{2}+1 \right) \left(n_{2}+2 \right)} + c_{n_{1}+2,n_{2}-2}^{*} c_{n_{1},n_{2}} \sqrt{n_{2} \left(n_{2}-1 \right) \left(n_{1}+1 \right) \left(n_{1}+2 \right)} \right) \\ &+ \frac{1}{4} \sum_{n_{1},n_{2}} |c_{n_{1},n_{2}}|^{2} \left(n_{2} \left(n_{1}+1 \right) + n_{1} \left(n_{2}+1 \right) \right) \\ \langle \left(\hat{J}_{y}^{(1,2)} \right) \rangle &= \frac{i}{2} \langle \left(\hat{a}_{1} \hat{a}_{2}^{\dagger} - \hat{a}_{1}^{\dagger} \hat{a}_{2} \right) \rangle = \frac{i}{2} \sum_{n_{1},n_{2}} \left(c_{n_{1}-1,n_{2}+1}^{*} c_{n_{1},n_{2}} \sqrt{n_{1} \left(n_{2}+1 \right)} - c_{n_{1}+1,n_{2}-1}^{*} c_{n_{1},n_{2}} \sqrt{n_{2} \left(n_{1}+1 \right)} \right). \end{split}$$

Using the definitions of \hat{p}_1 , \hat{p}_2 and their conjugates, i.e.,

$$\hat{x}_1 = \frac{1}{2} \left(\hat{a}_1 + \hat{a}_1^{\dagger} \right),$$

$$\hat{x}_2 = \frac{1}{2} \left(\hat{a}_2 + \hat{a}_2^{\dagger} \right),$$

we obtain

$$\Delta^2 \hat{J}_y^{(1,2)} = \langle (\hat{x}_1 \hat{p}_2 - \hat{p}_1 \hat{x}_2)^2 \rangle - (\langle \hat{x}_1 \hat{p}_2 - \hat{p}_1 \hat{x}_2 \rangle)^2 \,.$$

For the total variance we have

$$\begin{split} \Delta^2 \hat{J}_y^{(1,3)} + \Delta^2 \hat{J}_y^{(2,3)} + \Delta^2 \hat{J}_y^{(1,2)} &= N \Delta^2 \hat{p}_1 + N \Delta^2 \hat{p}_2 + \langle (\hat{x}_1 \hat{p}_2 - \hat{p}_1 \hat{x}_2)^2 \rangle - (\langle \hat{x}_1 \hat{p}_2 - \hat{p}_1 \hat{x}_2 \rangle)^2 \\ &= N \left(\Delta^2 \hat{p}_1 + \Delta^2 \hat{p}_2 + \frac{1}{N} \left(\langle (\hat{x}_1 \hat{p}_2 - \hat{p}_1 \hat{x}_2)^2 \rangle - (\langle \hat{x}_1 \hat{p}_2 - \hat{p}_1 \hat{x}_2 \rangle)^2 \right) \right) \\ &\underset{N \to \infty}{\approx} N \left(\Delta^2 \hat{p}_1 + \Delta^2 \hat{p}_2 \right). \end{split}$$

Thus, for estimating the variable χ , we obtain:

$$\delta\left(\frac{\chi}{2\sqrt{N}}\right) \ge \frac{1}{\sqrt{4\Delta^2 \hat{\kappa}_3}} = \frac{1}{2\sqrt{N\left(\Delta^2 \hat{p}_1 + \Delta^2 \hat{p}_2\right)}}$$
$$\delta\chi = \delta\left(2\sqrt{\left(\theta_{1,2}^2 + \theta_{1,3}^2 + \theta_{2,3}^2\right)}\right) \ge \frac{1}{\sqrt{\left(\Delta^2 \hat{p}_1 + \Delta^2 \hat{p}_2\right)}}.$$

Consequently, in the limit $N \to \infty$, the 3-mode estimation problem reduces to a two-mode continuous-variable problem. The highly populated third mode serves as a classical reference frame, while the remaining modes are described by canonical quadratures \hat{x}_i , \hat{p}_i . In this regime, the QFI accumulates contributions from each mode and the estimated parameter not only describes the rotation angle $\theta_{1,2}$ between these two modes but also the angles characterizing their rotation with respect to the reference mode.

At this limit, we can reformulate the collective generators in (52) using effective quadrature operators. Specifically, in the limit $N \to \infty$ the operators $\hat{J}_y^{(1,3)}$ and $\hat{J}_y^{(2,3)}$ become (up to a normalization) proportional to the quadratures \hat{p}_1 and \hat{p}_2 of the first two modes:

$$\hat{\kappa}_{2,\eta} = \cos \eta \, \frac{\hat{J}_y^{(1,3)}}{\sqrt{N}} + \sin \eta \, \frac{\hat{J}_y^{(2,3)}}{\sqrt{N}} \underset{N \to \infty}{\approx} \cos \eta \, \hat{p}_1 + \sin \eta \, \hat{p}_2, \tag{56a}$$

$$\hat{\kappa}_{1,\eta} = \sin \eta \, \frac{\hat{J}_y^{(1,3)}}{\sqrt{N}} - \cos \eta \, \frac{\hat{J}_y^{(2,3)}}{\sqrt{N}} \underset{N \to \infty}{\approx} \sin \eta \, \hat{p}_1 - \cos \eta \, \hat{p}_2. \tag{56b}$$

Then the collective generator in eq. (51) becomes

$$\hat{U} = e^{i\frac{\chi}{2}\hat{\kappa}_{2,\eta}},\tag{57}$$

and the variances satisfy the conserved sum

$$\Delta^2 \hat{\kappa}_{2,n} + \Delta^2 \hat{\kappa}_{1,n} = \Delta^2 \hat{p}_1 + \Delta^2 \hat{p}_2. \tag{58}$$

Therefore, to maximize the sensitivity (i.e., maximize the QFI associated with χ) we minimize the orthogonal variance $\Delta^2 \hat{\kappa}_{1,\eta} = 0$, since the precision limit associated with Eq. (57) becomes.

$$\delta\left(\frac{\chi}{2}\right) \ge \frac{1}{2\sqrt{\Delta^2 \hat{\kappa}_{2,\eta}}}.$$

As an example, we apply the above framework to the case of two modes, with each mode described by its associated quadrature operator \hat{p}_1 and \hat{p}_2 . We define the following collective operators:

$$\hat{p}_{+} = \frac{1}{\sqrt{2}} \left(\hat{p}_{1} + \hat{p}_{2} \right) \tag{59}$$

$$\hat{p}_{-} = \frac{1}{\sqrt{2}} \left(\hat{p}_{1} - \hat{p}_{2} \right), \tag{60}$$

Then the rotated operators in eq. (56) become

$$\hat{\kappa}_{2,\eta} = \cos \eta' \hat{p}_+ + \sin \eta' \, \hat{p}_-,\tag{61}$$

$$\hat{\kappa}_{1,\eta} = \cos \eta' \, \hat{p}_- - \sin \eta' \, \hat{p}_+, \tag{62}$$

where $\cos \eta' = \frac{1}{\sqrt{2}} (\sin \eta + \cos \eta)$ and $\sin \eta' = \frac{1}{\sqrt{2}} (\cos \eta - \sin \eta)$. With this, the unitary (57) is

$$\hat{U} = e^{i\frac{\chi}{2}\left(\cos\eta'\hat{p}_{+} + \sin\eta'\hat{p}_{-}\right)},\tag{63}$$

and the total variance (58) is still conserved:

$$\Delta^2 \hat{\kappa}_{2,\eta} + \Delta^2 \hat{\kappa}_{1,\eta} = \Delta^2 \hat{p}_+ + \Delta^2 \hat{p}_-. \tag{64}$$

For states for which $\Delta^2 \hat{p}_- = 0$, for instance, the best choice of evolution direction corresponds to $\sin \eta = \cos \eta = 1/\sqrt{2}$, $\hat{\kappa}_{2,\eta} = \hat{p}_+$, and the bound simplifies to:

$$\delta \chi \ge \frac{1}{\sqrt{\Delta^2 \hat{p}_+}}.$$

which is optimized for the given state. This shows that sensitivity to displacements along \hat{p}_+ improves with increasing $\Delta^2 \hat{p}_+$, which, due to the Heisenberg uncertainty principle, can be achieved by squeezing the quadrature $\frac{1}{\sqrt{2}}(\hat{x}_1 + \hat{x}_2)$ of the mode $\hat{a}_+ = \frac{1}{\sqrt{2}}(\hat{a}_1 + \hat{a}_2)$. This result can be generalized for different number of modes. Hence, in the CV limit, a correct mode choice for the evolution may improve the sensitivity to displacements, as studied in [99, 108]

Generalized measurement and optimal measurement strategy

In this section, following the results of Ref. [11], we discuss a scheme allowing to optimally estimate the parameter ζ , discussed in Sec. , for the probe state defined in (11). For such a 3-mode state, the scheme involves adding two auxiliary modes (mode 4 and 5) that are entangled, such that we have $|\text{aux}\rangle = \frac{1}{\sqrt{2}} (|0\rangle_4 |1\rangle_5 + |1\rangle_4 |0\rangle_5)$ and the state becomes

$$|\Psi\rangle = |\psi\rangle \otimes |\mathrm{aux}\rangle.$$

To extract information about the parameter ζ encoded via a unitary \hat{U} defined in (15) we apply \hat{U} in a conditional way, i.e., \hat{U} is applied to the probe if the auxiliary is in $|1\rangle_4|0\rangle_5$, and $\hat{S}\hat{U}$ if in $|0\rangle_4|1\rangle_5$. Here we defined a unitary operator \hat{S} such that $\hat{S}|\psi\rangle = \pm |\psi\rangle$ and it satisfies the condition $|\hat{S},\hat{U}| \neq 0$. The total evolved state becomes:

$$|\tilde{\Psi}\rangle = \frac{1}{\sqrt{2}} \left(\hat{U} |\psi\rangle \otimes |1\rangle_4 |0\rangle_5 + \hat{S}\hat{U} |\psi\rangle \otimes |0\rangle_4 |1\rangle_5 \right)$$
(65)

We now apply a beam splitter-like transformation to auxiliary modes, where in one arm of the balanced beam splitter the input is the mode $|1\rangle_4|0\rangle_5$ and on the other $|0\rangle_4|1\rangle_5$, thus after the beam splitter we obtain

$$\begin{split} |1\rangle_4|0\rangle_5 &\to \frac{1}{\sqrt{2}} \left(|1\rangle_4|0\rangle_5 + |0\rangle_4|1\rangle_5 \right) \\ |0\rangle_4|1\rangle_5 &\to \frac{1}{\sqrt{2}} \left(|1\rangle_4|0\rangle_5 - |0\rangle_4|1\rangle_5 \right), \end{split}$$

and the full state (65) after the beam splitter becomes

$$|\tilde{\Psi}\rangle = \frac{1}{2} \left(\left(\hat{U} + \hat{S}\hat{U} \right) |\psi\rangle \otimes |1\rangle_4 |0\rangle_5 + \left(\hat{U} - \hat{S}\hat{U} \right) |\psi\rangle \otimes |0\rangle_4 |1\rangle_5 \right).$$

Finally, we make a measurement on a basis of the auxiliary modes, then the probability of detecting $|1\rangle_4|0\rangle_5$ is

$$p_{10} = \frac{1}{4} \langle \psi | \left(U^{\dagger} + U^{\dagger} S^{\dagger} \right) \left(U + S U \right) | \psi \rangle = \frac{1}{4} \langle \psi | \left(2I + U^{\dagger} S U + U^{\dagger} S^{\dagger} U \right) | \psi \rangle$$
$$= \frac{1}{2} \langle \psi | \left(I + \operatorname{Re} \left\{ U^{\dagger} S U \right\} \right) | \psi \rangle = \frac{1}{2} + \frac{1}{2} \langle \psi | \operatorname{Re} \left\{ U^{\dagger} S U \right\} | \psi \rangle,$$

where I is the identity operator and Re $\{\cdot\}$ denotes the real part of the operator. Similarly, the probability of detecting $|0\rangle_4|1\rangle_5$ is

$$p_{01} = \frac{1}{2} - \frac{1}{2} \langle \psi | \operatorname{Re} \left\{ U^{\dagger} S U \right\} | \psi \rangle.$$

Recalling that we study a unitary given by $\hat{U} = e^{i\frac{\hat{\zeta}}{2}\hat{\kappa}_3}$, we refer to the results of Ref. [11], which show that for a measurement to be the optimal one, the measurement operator \hat{S} must anticommute with the generator of the

unitary: $\{\hat{\kappa}_3, \hat{S}\} = \hat{\kappa}_3 \hat{S} + \hat{S} \hat{\kappa}_3 = 0$. This anticommutation condition ensures that \hat{S} is an optimal observable for estimating the parameter ζ in the sense that the measurement of \hat{S} on the evolved state extracts the maximum amount of Fisher information, i.e., the quantum Fisher information.

Expanding this using the expression from Eq. (13a), we obtain:

$$\{\hat{\kappa}_3, \hat{S}\} = \cos \phi_2 \{\hat{n}_3, \hat{S}\} + \sin \phi_2 \left(\cos \phi_1 \{\hat{n}_2, \hat{S}\} + \sin \phi_1 \{\hat{n}_1, \hat{S}\}\right) = 0.$$

Using photon number conservation $\hat{n}_3 = N - (\hat{n}_1 + \hat{n}_2)$, the above expression becomes

$$(\cos\phi_2 - \sin\phi_2\cos\phi_1)\{\hat{n}_2, \hat{S}\} + (\cos\phi_2 - \sin\phi_2\sin\phi_1)\{\hat{n}_1, \hat{S}\} = 2N\cos\phi_2\hat{S}. \tag{66}$$

If we consider the special case where the first two modes contain equal photon numbers, $n_1 = n_2 = n$, and use the parameters $\sin \phi_1 = \cos \phi_1 = 1/\sqrt{2}$, $\sin \phi_2 = 1/\sqrt{3}$ and $\cos \phi_2 = -\sqrt{2/3}$, as derived in Sec. , the condition (66) simplifies to

$$\{\hat{n}, \hat{S}\} = \frac{2}{3}N\hat{S}.\tag{67}$$

By finding the operator \hat{S} satisfying this condition, we ensure that the QFI derived in Sec. , corresponding to $\Delta^2 \hat{\kappa}_3$ is attained.

As an example, consider a symmetry operator \hat{S} that acts on the first two modes:

$$\hat{S} = \sum_{n=0}^{\lfloor N/2 \rfloor} s_n |n\rangle_1 |n\rangle_2 \langle n|_1 \langle n|_2, \tag{68}$$

where $s_n = (-1)^{f(n)}$, where $f \in \mathcal{F}(\mathbb{N}, \mathbb{N})$, such that the condition $\hat{S}|\psi\rangle = \pm |\psi\rangle$ is satisfied. One example of such a function is f(n) = n. Computing the anticommutator:

$$\{\hat{n}, \hat{S}\} = \sum_{n=0}^{\lfloor N/2 \rfloor} s_n \left(\hat{n} | n \rangle_1 | n \rangle_2 \langle n |_1 \langle n |_2 + | n \rangle_1 | n \rangle_2 \langle n |_1 \langle n |_2 \hat{n} \right) = \sum_{n=0}^{\lfloor N/2 \rfloor} 2s_n n | n \rangle_1 | n \rangle_2 \langle n |_1 \langle n |_2, \tag{69}$$

and comparing it with the right-hand side of eq. (67):

$$\frac{2}{3}N\hat{S} = \frac{2}{3}N\sum_{n=0}^{\lfloor N/2\rfloor} s_n |n\rangle_1 |n\rangle_2 \langle n|_1 \langle n|_2, \tag{70}$$

we find that the condition (67) is satisfied when $n = \frac{N}{3}$. We note that in systems where the reference frame corresponds to the limit $N \to \infty$, this condition on n becomes unphysical.

^{*} corresponding author: perola.milman@u-paris.fr

^[1] V. Giovannetti, S. Lloyd, and L. Maccone, Quantum-enhanced measurements: Beating the standard quantum limit, Science 306, 1330 (2004), https://www.science.org/doi/pdf/10.1126/science.1104149.

^[2] V. Giovannetti, S. Lloyd, and L. Maccone, Quantum metrology, Phys. Rev. Lett. 96, 010401 (2006).

^[3] B. P. Abbott and *et al.* (LIGO Scientific Collaboration and Virgo Collaboration), Observation of gravitational waves from a binary black hole merger, Phys. Rev. Lett. **116**, 061102 (2016).

^[4] K. C. Toussaint, G. Di Giuseppe, K. J. Bycenski, A. V. Sergienko, B. E. A. Saleh, and M. C. Teich, Quantum ellipsometry using correlated-photon beams, Phys. Rev. A 70, 023801 (2004).

^[5] J. A. Jones, S. D. Karlen, J. Fitzsimons, A. Ardavan, S. C. Benjamin, G. A. D. Briggs, and J. J. L. Morton, Magnetic field sensing beyond the standard quantum limit using 10-spin noon states, Science 324, 1166 (2009), https://www.science.org/doi/pdf/10.1126/science.1170730.

^[6] M. A. Taylor and W. P. Bowen, Quantum metrology and its application in biology, Physics Reports 615, 1 (2016), quantum metrology and its application in biology.

^[7] A. Crespi, M. Lobino, J. C. F. Matthews, A. Politi, C. R. Neal, R. Ramponi, R. Osellame, and J. L. O'Brien, Measuring protein concentration with entangled photons, Applied Physics Letters 100, 233704 (2012), https://pubs.aip.org/aip/apl/article-pdf/doi/10.1063/1.4724105/14251724/233704_1_online.pdf.

- [8] K. R. Motes, J. P. Olson, E. J. Rabeaux, J. P. Dowling, S. J. Olson, and P. P. Rohde, Linear optical quantum metrology with single photons: Exploiting spontaneously generated entanglement to beat the shot-noise limit, Phys. Rev. Lett. 114, 170802 (2015).
- [9] V. Giovannetti, S. Lloyd, and L. Maccone, Quantum-enhanced positioning and clock synchronization, Nature 412, 417 (2001).
- [10] E. Descamps, N. Fabre, A. Keller, and P. Milman, Quantum metrology using time-frequency as quantum continuous variables: Resources, sub-shot-noise precision and phase space representation, Phys. Rev. Lett. 131, 030801 (2023).
- [11] E. Descamps, A. Keller, and P. Milman, Time-frequency metrology with two single-photon states: Phase-space picture and the hong-ou-mandel interferometer, Phys. Rev. A 108, 013707 (2023).
- [12] L. Pezzé and A. Smerzi, Mach-zehnder interferometry at the Heisenberg limit with coherent and squeezed-vacuum light, Phys. Rev. Lett. 100, 073601 (2008).
- [13] J. P. Dowling, Quantum optical metrology the lowdown on high-n00n states, Contemporary Physics 49, 125 (2008).
- [14] E. Polino, M. Valeri, N. Spagnolo, and F. Sciarrino, Photonic quantum metrology, AVS Quantum Science 2, 024703 (2020).
- [15] K. Duivenvoorden, B. M. Terhal, and D. Weigand, Single-mode displacement sensor, Physical Review A 95, 012305 (2017).
- [16] M. Fadel, N. Roux, and M. Gessner, Quantum metrology with a continuous-variable system (2024), arXiv:2411.04122 [quant-ph].
- [17] M. J. Holland and K. Burnett, Interferometric detection of optical phase shifts at the heisenberg limit, Physical Review Letters 71, 1355 (1993).
- [18] H. Kwon, Y. Lim, L. Jiang, H. Jeong, and C. Oh, Quantum metrological power of continuous-variable quantum networks, Physical Review Letters 128, 180503 (2022).
- [19] O. Pinel, J. Fade, D. Braun, P. Jian, N. Treps, and C. Fabre, Ultimate sensitivity of precision measurements with Gaussian quantum light: a multi-modal approach, Phys. Rev. A 85, 010101 (2012), 1105.2644.
- [20] L. Pezzè, A. Smerzi, M. K. Oberthaler, R. Schmied, and P. Treutlein, Quantum metrology with nonclassical states of atomic ensembles, Rev. Mod. Phys. 90, 035005 (2018).
- [21] A. Sinatra, Spin-squeezed states for metrology, Applied Physics Letters **120**, 120501 (2022), https://pubs.aip.org/aip/apl/article-pdf/doi/10.1063/5.0084096/20034807/120501_1_5.0084096.pdf.
- [22] J. Zhang, M. Um, D. Lv, J.-N. Zhang, L.-M. Duan, and K. Kim, Noon states of nine quantized vibrations in two radial modes of a trapped ion, Phys. Rev. Lett. 121, 160502 (2018).
- [23] S. Qvarfort, A. Serafini, P. F. Barker, and S. Bose, Gravimetry through non-linear optomechanics, Nature Communications 9, 1 (2018).
- [24] V. Giovannetti, S. Lloyd, and L. Maccone, Advances in quantum metrology, Nature Photon. 5, 222 (2011), arXiv:1102.2318 [quant-ph].
- [25] F. Benatti, R. Floreanini, and U. Marzolino, Sub-shot-noise quantum metrology with entangled identical particles, Annals of Physics 325, 924 (2010).
- [26] B. J. Dalton, L. Heaney, J. Goold, B. M. Garraway, and T. Busch, New spin squeezing and other entanglement tests for two mode systems of identical bosons, New Journal of Physics 16, 013026 (2014).
- [27] J. Sahota, N. Quesada, and D. F. V. James, Physical resources for optical phase estimation, Phys. Rev. A 94, 033817 (2016).
- [28] D. Šafránek, Estimation of gaussian quantum states, Journal of Physics A: Mathematical and Theoretical 52, 035304 (2018).
- [29] B. Yurke, S. L. McCall, and J. R. Klauder, Su(2) and su(1,1) interferometers, Phys. Rev. A 33, 4033 (1986).
- [30] L. Maccone and A. Riccardi, Squeezing metrology: a unified framework, Quantum 4, 292 (2020).
- [31] B. C. Sanders, S. D. Bartlett, T. Rudolph, and P. L. Knight, Photon-number superselection and the entangled coherentstate representation, Phys. Rev. A 68, 042329 (2003).
- [32] K. Mølmer, Optical coherence: A convenient fiction, Phys. Rev. A 55, 3195 (1997).
- [33] J. Gea-Banacloche, Comment on "optical coherence: A convenient fiction", Phys. Rev. A 58, 4244 (1998).
- [34] K. Mølmer, Reply to "comment on 'optical coherence: A convenient fiction", Phys. Rev. A 58, 4247 (1998).
- [35] S. D. Bartlett, T. Rudolph, and R. W. Spekkens, Dialogue concerning two views on quantum coherence: Factist and fictionist, International Journal of Quantum Information **04**, 17 (2006), https://doi.org/10.1142/S0219749906001591.
- [36] B. C. Sanders, Review of entangled coherent states, Journal of Physics A: Mathematical and Theoretical 45, 244002 (2012).
- [37] Y. Aharonov and L. Susskind, Charge superselection rule, Phys. Rev. 155, 1428 (1967).
- [38] D. N. Page and W. K. Wootters, Evolution without evolution: Dynamics described by stationary observables, Phys. Rev. D 27, 2885 (1983).
- [39] S. D. Bartlett, T. Rudolph, and R. W. Spekkens, Reference frames, superselection rules, and quantum information, Rev. Mod. Phys. 79, 555 (2007).
- [40] E. Descamps, A. Saharyan, A. Chivet, A. Keller, and P. Milman, Modes, states and superselection rules in quantum optics and quantum information (2025), arXiv:2501.03943 [quant-ph].
- [41] E. Descamps, N. Fabre, A. Saharyan, A. Keller, and P. Milman, Superselection rules and bosonic quantum computational resources, Phys. Rev. Lett. 133, 260605 (2024).
- [42] J. R. Hervas, A. Z. Goldberg, A. S. Sanz, Z. Hradil, J. Řeháček, and L. L. Sánchez-Soto, Beyond the quantum cramér-rao bound, Phys. Rev. Lett. 134, 010804 (2025).

- [43] J. Wang, L. Davidovich, and G. S. Agarwal, Quantum sensing of open systems: Estimation of damping constants and temperature, Phys. Rev. Res. 2, 033389 (2020).
- [44] J. Wang, R. L. d. M. Filho, G. S. Agarwal, and L. Davidovich, Quantum advantage of time-reversed ancilla-based metrology of absorption parameters, Phys. Rev. Res. 6, 013034 (2024).
- [45] M. Kacprowicz, R. Demkowicz-Dobrzański, W. Wasilewski, K. Banaszek, and I. A. Walmsley, Experimental quantum-enhanced estimation of a lossy phase shift, Nature Photonics 4, 357 (2010), arXiv:0906.3511 [quant-ph].
- [46] O. Meskine, E. Descamps, A. Keller, A. Lemaître, F. Baboux, S. Ducci, and P. Milman, Approaching maximal precision of hong-ou-mandel interferometry with nonperfect visibility, Phys. Rev. Lett. 132, 193603 (2024).
- [47] J.-G. Baak and U. R. Fischer, Classical and quantum metrology of the lieb-liniger model, Phys. Rev. A 106, 062442 (2022).
- [48] B. Escher, R. de Matos Filho, and L. Davidovich, General framework for estimating the ultimate precision limit in noisy quantum-enhanced metrology, Nature Physics 7, 406 (2001).
- [49] X. Wang and B. C. Sanders, Relations between bosonic quadrature squeezing and atomic spin squeezing, Phys. Rev. A 68, 033821 (2003).
- [50] M. Ozawa, Measurement breaking the standard quantum limit for free-mass position, Phys. Rev. Lett. 60, 385 (1988).
- [51] A. Z. Goldberg and D. F. V. James, Quantum-limited euler angle measurements using anticoherent states, Phys. Rev. A 98, 032113 (2018).
- [52] J. Martin, S. Weigert, and O. Giraud, Optimal Detection of Rotations about Unknown Axes by Coherent and Anticoherent States, Quantum 4, 285 (2020).
- [53] R. H. Dicke, Coherence in spontaneous radiation processes, Phys. Rev. 93, 99 (1954).
- [54] Z. Zhang and L. M. Duan, Quantum metrology with dicke squeezed states, New Journal of Physics 16, 103037 (2014).
- [55] F. Bouchard, P. de la Hoz, G. Björk, R. W. Boyd, M. Grassl, Z. Hradil, E. Karimi, A. B. Klimov, G. Leuchs, J. Řeháček, and L. L. Sánchez-Soto, Quantum metrology at the limit with extremal majorana constellations, Optica 4, 1429 (2017).
- [56] V. D'Ambrosio, N. Spagnolo, L. Del Re, S. Slussarenko, Y. Li, L. Kwek, L. Marrucci, S. Walborn, L. Aolita, and F. Sciarrino, Photonic polarization gears for ultra-sensitive angular measurements, Nature communications 4, 2432 (2013).
- [57] M. Mitchell, J. Lundeen, and A. Steinberg, Super-resolving phase measurements with a multiphoton entangled state, Nature 429, 161 (2004).
- [58] L. Pezzé and A. Smerzi, Quantum theory of phase estimation, Atom Interferometry 188 (2014).
- [59] M. Reisner, F. Mazeas, R. Dauliat, B. Leconte, D. Aktas, R. Cannon, P. Roy, R. Jamier, G. Sauder, F. Kaiser, S. Tanzilli, and L. Labonté, Quantum-limited determination of refractive index difference by means of entanglement, npj Quantum Inf., 58 (2022).
- [60] F. Toscano, D. A. R. Dalvit, L. Davidovich, and W. H. Zurek, Sub-Planck phase-space structures and Heisenberg-limited measurements, Phys. Rev. A 73, 023803 (2006).
- [61] W. H. Zurek, Sub-Planck structure in phase space and its relevance for quantum decoherence, Nature 412, 712 (2001).
- [62] D. A. R. Dalvit, R. L. de Matos Filho, and F. Toscano, Quantum metrology at the Heisenberg limit with ion trap motional compass states, New Journal of Physics 8, 276 (2006).
- [63] R. Demkowicz-Dobrzański, M. Jarzyna, and J. Kołodyński, Chapter four quantum limits in optical interferometry (Elsevier, 2015) pp. 345–435.
- [64] D. Braun, G. Adesso, F. Benatti, R. Floreanini, U. Marzolino, M. W. Mitchell, and S. Pirandola, Quantum-enhanced measurements without entanglement, Reviews of Modern Physics 90, 035006 (2018).
- [65] I. Frérot and T. Roscilde, Symmetry: A fundamental resource for quantum coherence and metrology, Phys. Rev. Lett. 133, 260402 (2024).
- [66] B. Morris, B. Yadin, M. Fadel, T. Zibold, P. Treutlein, and G. Adesso, Entanglement between identical particles is a useful and consistent resource, Phys. Rev. X 10, 041012 (2020).
- [67] J. Schwinger, Angular momentum, in Quantum Mechanics: Symbolism of Atomic Measurements, edited by B.-G. Englert (Springer Berlin Heidelberg, Berlin, Heidelberg, 2001) pp. 149–181.
- [68] K. P. Seshadreesan, S. Kim, J. P. Dowling, and H. Lee, Phase estimation at the quantum Cramér-Rao bound via parity detection, Phys. Rev. A 87, 043833 (2013).
- [69] Q. Zhuang, J. Preskill, and L. Jiang, Distributed quantum sensing enhanced by continuous-variable error correction, New Journal of Physics 22, 022001 (2020).
- [70] M. Tse and et al. (LIGO Scientific Collaboration and Virgo Collaboration), Quantum-enhanced advanced ligo detectors in the era of gravitational-wave astronomy, Phys. Rev. Lett. 123, 231107 (2019).
- [71] M. Penasa, S. Gerlich, T. Rybarczyk, V. Métillon, M. Brune, J. M. Raimond, S. Haroche, L. Davidovich, and I. Dotsenko, Measurement of a microwave field amplitude beyond the standard quantum limit, Phys. Rev. A **94**, 022313 (2016).
- [72] W. H. Zurek, Sub-Planck structure in phase space and its relevance for quantum decoherence, Nature 412, 712 (2001).
- [73] See supplementary material [url].
- [74] where we supposed for simplifying reasons and without loss of generality, as we will discuss later, that the two modes have the same frequency ω ().
- [75] L.-M. Duan, J. I. Cirac, and P. Zoller, Quantum entanglement in spinor bose-einstein condensates, Phys. Rev. A 65, 033619 (2002).
- [76] T. Holstein and H. Primakoff, Field dependence of the intrinsic domain magnetization of a ferromagnet, Phys. Rev. 58, 1098 (1940).
- [77] However, even if introducing constraints is not fundamentally necessary, this strategy can be, in practice, applied to further reduce the space dimension and to provide insights about the interplay between different controllable resources,

- as time and energy [?]. ().
- [78] N. Gutman, A. Gorlach, O. Tziperman, R. Ruimy, and I. Kaminer, Universal control of symmetric states using spin squeezing, Phys. Rev. Lett. 132, 153601 (2024).
- [79] D. J. Wineland, J. J. Bollinger, W. M. Itano, F. L. Moore, and D. J. Heinzen, Spin squeezing and reduced quantum noise in spectroscopy, Phys. Rev. A 46, R6797 (1992).
- [80] D. J. Wineland, J. J. Bollinger, W. M. Itano, and D. J. Heinzen, Squeezed atomic states and projection noise in spectroscopy, Phys. Rev. A 50, 67 (1994).
- [81] C. Gross, Spin squeezing, entanglement and quantum metrology with bose–einstein condensates, Journal of Physics B: Atomic, Molecular and Optical Physics 45, 103001 (2012).
- [82] A. S. Sørensen and K. Mølmer, Entanglement and extreme spin squeezing, Phys. Rev. Lett. 86, 4431 (2001).
- [83] S. L. Braunstein and P. van Loock, Quantum information with continuous variables, Rev. Mod. Phys. 77, 513 (2005), quant-ph/0410100.
- [84] C. Fabre and N. Treps, Modes and states in quantum optics, Rev. Mod. Phys. 92, 035005 (2020).
- [85] L. MANDEL and E. WOLF, Coherence properties of optical fields, Rev. Mod. Phys. 37, 231 (1965)
- [86] J.-G. Baak and U. R. Fischer, Self-consistent many-body metrology, Phys. Rev. Lett. 132, 240803 (2024).
- [87] S. Lloyd and S. L. Braunstein, Quantum computation over continuous variables, Phys. Rev. Lett. 82, 1784 (1999).
- [88] N. Killoran, M. Cramer, and M. B. Plenio, Extracting entanglement from identical particles, Phys. Rev. Lett. 112, 150501 (2014).
- [89] T. Holstein and H. Primakoff, Field dependence of the intrinsic domain magnetization of a ferromagnet, Phys. Rev. 58, 1098 (1940).
- [90] T. J. Volkoff and K. B. Whaley, Measurement- and comparison-based sizes of schrödinger cat states of light, Phys. Rev. A 89, 012122 (2014).
- [91] J. Huang, M. Zhuang, B. Lu, Y. Ke, and C. Lee, Achieving heisenberg-limited metrology with spin cat states via interaction-based readout, Phys. Rev. A 98, 012129 (2018).
- [92] Y. Maleki, M. O. Scully, and A. M. Zheltikov, Quantum metrology with superposition spin coherent states: Insights from fisher information, Phys. Rev. A **104**, 053712 (2021).
- [93] B. C. Sanders, Quantum dynamics of the nonlinear rotator and the effects of continual spin measurement, Phys. Rev. A 40, 2417 (1989).
- [94] U. R. Fischer and M.-K. Kang, "photonic" cat states from strongly interacting matter waves, Phys. Rev. Lett. 115, 260404 (2015).
- [95] B. C. Sanders and C. C. Gerry, Connection between the noon state and a superposition of su(2) coherent states, Phys. Rev. A 90, 045804 (2014).
- [96] J. Wang, R. L. d. M. Filho, G. S. Agarwal, and L. Davidovich, Quantum advantage of time-reversed ancilla-based metrology of absorption parameters, Phys. Rev. Res. 6, 013034 (2024).
- [97] H. F. Hofmann, All path-symmetric pure states achieve their maximal phase sensitivity in conventional two-path interferometry, Phys. Rev. A 79, 033822 (2009).
- [98] E. Descamps, A. Keller, and P. Milman, Time-frequency metrology with two single-photon states: Phase-space picture and the hong-ou-mandel interferometer, Phys. Rev. A 108, 013707 (2023).
- [99] M. Gessner, N. Treps, and C. Fabre, Estimation of a parameter encoded in the modal structure of a light beam: a quantum theory, Optica 10, 996 (2023).
- [100] P. Hyllus, O. Gühne, and A. Smerzi, Not all pure entangled states are useful for sub-shot-noise interferometry, Phys. Rev. A 82, 012337 (2010).
- [101] E. Descamps, A. Keller, and P. Milman, Measuring entanglement along collective operators, Phys. Rev. A 111, 052428 (2025).
- [102] A. Lyons, G. C. Knee, E. Bolduc, T. Roger, J. Leach, E. M. Gauger, and D. Faccio, Attosecond-resolution Hong-Ou-Mandel interferometry, Sci. Adv. 4, eaap9416 (2018).
- [103] S. J. Johnson, C. P. Lualdi, A. P. Conrad, N. T. Arnold, M. Vayninger, and P. G. Kwiat, Toward vibration measurement via frequency-entangled two-photon interferometry, in *Quantum Sensing, Imaging, and Precision Metrology*, Vol. 12447, edited by J. Scheuer and S. M. Shahriar, International Society for Optics and Photonics (SPIE, 2023) p. 124471C.
- [104] Y. Chen, M. Fink, F. Steinlechner, J. P. Torres, and R. Ursin, Hong-Ou-Mandel interferometry on a biphoton beat note, npj Quantum Information 5, 43 (2019).
- [105] G. Tóth, Multipartite entanglement and high-precision metrology, Physical Review A 85, 10.1103/physreva.85.022322 (2012).
- [106] A. Sørensen, L.-M. Duan, J. I. Cirac, and P. Zoller, Many-particle entanglement with bose–einstein condensates, Nature 409, 63 (2001).
- [107] A. Hertz, N. J. Cerf, and S. De Bièvre, Relating the entanglement and optical nonclassicality of multimode states of a bosonic quantum field, Phys. Rev. A 102, 032413 (2020).
- [108] O. Pinel, J. Fade, D. Braun, P. Jian, N. Treps, and C. Fabre, Ultimate sensitivity of precision measurements with intense gaussian quantum light: A multimodal approach, Phys. Rev. A 85, 010101 (2012).